2020-01-01

# Analyzing ZNF16: An Understudied Gene

Chelsea L. George
*University of Texas at El Paso*

ANALYZING ZNF16: AN UNDERSTUDIED GENE

CHELSEA L. GEORGE

Master's Program in Biological Sciences

APPROVED:

Siddhartha Das, Ph.D., Chair

Laura A. Diaz-Martinez, Ph.D.

Anita Quintana, Ph.D.

Giulio Francia, Ph.D.

Stephen Crites, Ph.D.
Dean of the Graduate School

# ANALYZING ZNF16: AN UNDERSTUDIED GENE

by

CHELSEA L. GEORGE, B.S.

THESIS

Presented to the Faculty of the Graduate School of

The University of Texas at El Paso

in Partial Fulfillment

of the Requirements

for the Degree of

MASTER OF SCIENCE

Department of Biological Sciences

THE UNIVERSITY OF TEXAS AT EL PASO

May 2020

ACKNOWLEDGEMENTS

I would like to thank Dr. Laura Diaz-Martinez for the time, advice, and encouragement she has poured into this project. She is an incredible mentor and I am honored to have had the chance to learn from her. We thank Dr. Sid Das for his support, Dr. Armando Varela for help with microscopy, and Gladys Almodovar for help with cell culture. Additionally, we would like to thank Igor Estevao for help with various instruments, Dr. Luis Martinez for use of his microscope, Arlene Levario for the stable EGFP-ZNF16 cell line, Colin Knight for help with the X-RAD 160, Dr. Sukla Roychowdhury for materials, and fellow lab mates for helpful discussions. This project was funded by: URI Grant #14-6486-39 and BD Biosciences Cancer Research Grant. The UTEP BBRC Core Facility is supported by grant #BBRC:5612MD007592

ABSTRACT

The zinc finger protein 16 (ZNF16) has been reported to be involved in megakaryocytic and erythroid differentiation. However, ZNF16 has ubiquitous expression throughout the body thus suggesting that it might have functions outside of these blood cell lineages. Here we show that ZNF16 is expressed in different tumor and non-tumor cell lines, consistent with the hypothesis of a more widespread role. Endogenous ZNF16 localizes to the nucleus and is enriched in the nucleolus. Interestingly, exogenous ZNF16 showed two patterns of localization depending on the tag used. EGFP-ZNF16 showed nuclear localization while 3xEGFP-ZNF16 was mainly localized to the nucleoli and other subnuclear structures. Given that endogenous ZNF16 localizes to both the nucleus and the nucleolus, the difference in localization of tagged ZNF16 likely is the result of preferential localization depending on the tag used. Based on its enrichment at the nucleolus, we tested for a role of ZNF16 in rRNA transcription and nucleolar stress. Results show that overexpression of ZNF16 targeted to the nucleolus results in increased rDNA transcription and that ZNF16 delocalizes from the nucleolus in conditions of nucleolar stress. These results indicate that ZNF16 is involved in rRNA synthesis. Lastly, we sought to test for a potential role for ZNF16 in the response to DNA damage. Our results show a potential yet minor involvement for ZNF16 in this process that depends on the cell line and type of DNA damage used. Together, these results reveal potential roles for ZNF16 in basic cellular processes, consistent with its ubiquitous expression in human tissues. Further characterization at the cellular and molecular level will offer insight on the function of this poorly characterized gene.

TABLE OF CONTENTS

# CHAPTER 1: INTRODUCTION

The rapid development of functional genetics and functional genomics approaches to study gene function has led to the accumulation of large datasets with information about the potential roles for thousands of genes in important cellular functions. As of April of 2019, a search in PubMed using the term 'genome-wide screen' identified more than 4000 reports using these approaches. Each of those screens provides data for tens of thousands of genes. Due to the amount of data generated in these screens, the noise levels inherent in these studies is large. A common approach used to narrow down the number of candidates for further study is to combine the results of the screen with already existing information about each gene (e.g., Gene Ontology, protein-protein interaction databases, molecular pathways knowledge) (Huang et al., 2008). Combining this information allows the identification of networks of genes to be involved in the specific function being studied and reduces the number of false positives, based on the premise that the likelihood of gene A being involved in a process is higher if gene B, a known interactor of gene A, is also identified in the screen. However, this approach has the caveat of overlooking genes for which little information exists in other databases.

Here I propose an approach to study the cellular and molecular function of the gene, zinc finger protein 16 (ZNF16), a poorly characterized gene that was identified as a potential regulator of survival to taxol in a genome-wide siRNA screen (Díaz-Martínez et al., 2014). Taxol, commonly used to treat a variety of cancers (Weaver, 2014), induces mitotic arrest (Hruban et al., 1989) through the stabilization of microtubules (Schiff et al., 1979). In studies exploring taxol and its antitumor activity, it is reported that many tumor cells arrested in mitosis by taxol die by apoptosis (Milas et al., 1995). HeLa cells treated with four separate siRNAs for ZNF16 each showed increased survival in taxol and fewer cells halted in mitosis compared with

controls. Additional analysis showed that ZNF16 siRNAs induced rapid exit from the mitotic arrest, suggesting that ZNF16-depleted cells had defects in the spindle checkpoint, leading to resistance to taxol (Diaz-Martinez, unpublished).

Despite the promising results indicating that ZNF16 might be important for the response to taxol, this gene was not chosen for further study in the original project because it was not included in any of the gene networks identified during the secondary analysis of the data using Ingenuity Pathways (Díaz-Martínez et al., 2014). Since ZNF16 is a gene that has been poorly characterized, we believe it might have been overlooked during the secondary analysis due to its lack of known interactions with defined gene networks. This highlights the need to study poorly characterized genes to better understand their functions.

*ZNF16: a gene of the $C_2H_2$ Zinc Finger Protein Family*

ZNF16 belongs to the $C_2H_2$ zinc finger protein family (Peng et al., 2006) which is one of the largest classes of human transcription factors (Najafabadi et al., 2015). The $C_2H_2$ zinc finger motif is a small (28-30 amino acids) protein structure characterized by its ability to bind a zinc ion through interactions with two cysteine and two histidine residues. The domain is folded into finger-like structures that were originally identified as DNA-binding motifs (Collins et al., 2001). This prominent family of proteins is widely distributed within eukaryotic genomes, with the $C_2H_2$ domain being one of the most common protein domains in eukaryotes. This motif is found across all kingdoms and is estimated to be the second most predominant protein domain in humans (Brayer and Segal, 2008).

In a study examining the in vivo binding of $C_2H_2$ zinc finger proteins to DNA, it was indicated that $C_2H_2$ zinc finger proteins recognize more motifs than all other human transcription

factors combined (Najafabadi et al., 2015). This widespread recognition is linked to the possible variation found within the $C_2H_2$ zinc finger protein family. The precise binding properties of a zinc finger protein to DNA, RNA, or proteins, are determined by the class of $C_2H_2$ zinc finger proteins (Iuchi, 2001a) as well as the number of $C_2H_2$ zinc fingers, amino acid sequence of the finger domain, and linker between fingers (Iuchi, 2001b) and can be highly specific to their targets (Brown, 2005).

Despite their widespread recognition as transcription regulators, zinc finger motifs were later shown to also bind RNA and mediate protein-protein interactions (Brayer and Segal, 2008). It is generally reported that as the number of zinc fingers increases in a protein, the number of fingers with specific affinity for ligands other than DNA also increases (Iuchi, 2001a). Not surprisingly, zinc finger proteins are involved in numerous cellular processes such as the regulation of transcription, ubiquitin-mediated protein degradation, signal transduction, DNA repair, and cell migration (Cassandri et al., 2017).

*ZNF16 gene structure and expression*

ZNF16 is located at the end of chromosome 8 (8q24.3), in a region that harbors a cluster of seven zinc finger proteins. However, ZNF16 is unique compared to its neighbors. Unlike its six neighbors, ZNF16 lacks the Krüppel-associated box (KRAB) (Lorenz et al., 2010), a domain that often functions as a transcriptional repressor (Urrutia, 2003). The ZNF16 gene is encoded on the complementary strand, is transcribed towards the centromere (Lorenz et al., 2010), contains five exons, and two alternatively spliced forms have been identified. ZNF16 mRNA is ubiquitously expressed across various tissues with reports of high expression in the thyroid,

prostate, kidney and uterus (NCBI) as well as in the brain, heart, skeletal muscle, liver (Peng et al., 2006) and fetal brain, testis, cerebellum and kidney (Lorenz et al., 2010).

Additionally, ZNF16 mRNA is expressed in a wide range of cell lines with the highest expression in cell lines from the breast, female reproductive system, renal system, urinary system, male reproductive system, and brain, as reported by the Cell Atlas (Uhlén et al., 2015). Little is known about the transcriptional control of ZNF16 expression. A single report addressing this topic found through a luciferase reporter system and chromatin immunoprecipitation, that MEF2A, a protein involved in the regulatory function of skeletal muscle, cardiac muscle, immune cells, and neuronal cells, binds to the regulatory region of ZNF16, positively regulating ZNF16 expression (Liu et al., 2011).

*ZNF16 protein structure and conservation*

Databases such as NCBI and OrthoDB list ZNF16 orthologs in 75+ species including mammalian and non-mammalian organisms such as *Xenopus laevis*. However, given that zinc fingers are a common protein domain, it is possible that some of these hits are not true ZNF16 orthologs but simply orthologs for other zinc finger proteins. A detailed study of the locus of zinc finger proteins found at 8q24.3, which harbors ZNF16, showed that the cluster is conserved in placental mammals (Lorenz et al., 2010). Interestingly, ZNF16 is conserved in humans, rhesus monkeys, dogs and cows, but seems to be a pseudogene in mice and rats (Lorenz et al., 2010).

ZNF16 has 17 zinc fingers at the C-terminus, the first two zinc fingers are $C_2H_2$ atypical, while the remaining 15 are of typical $C_2H_2$ zinc finger characterization (UniProt). Comparison of the ZNF16 protein sequence with all other human proteins shows that the N-terminal region of ZNF16 is relatively unique (Cell Atlas; Uhlén et al., 2015), without any conserved domains

(Lorenz et al., 2010). However, a study that fused different regions of ZNF16 to the GAL4-DNA binding domain revealed that a region in the ZNF16 N-terminus (aa 49-197) can function as a transcriptional activator (Deng et al., 2009).

Information about ZNF16 interactions with other proteins is scarce. A study has reported identification of ZNF16 binding partners by using a yeast two-hybrid screen (Li et al., 2011). This analysis identified 29 potential interactors, including proteins involved in differentiation of blood cells (e.g., EPB42, DEFA1, ZXDC) and the cell cycle protein, INCA1. The authors confirmed the INCA1-ZNF16 interaction by co-immunoprecipitation and observed a slight increase of cells in G2 in K562 cells overexpressing ZNF16 (Li et al., 2011). It has also been reported through chromatography and mass spectrometry approaches that ZNF16 is associated with 2 variants of linker histone H1 involved in the formation and stabilization of chromatin structures as well as the regulation of gene expression (Zhang et al., 2016).

Information found on interaction databases is also limited. For example, the BioGRID (v. 3.5) lists eight interactors for ZNF16: the Golgi protein GORAB, the zinc finger protein ZNF101, histone HIST1H1E, the nucleolar protein GLTSCR2, the ring finger proteins RNF151 and RNF4, the estrogen receptor ESR2, and PPAN, a protein involved in rRNA maturation. All of these interactions are derived from high-throughput methods such as genome-wide yeast two-hybrid and proteome-wide high affinity purification followed by mass spectrometry and have not been confirmed by other means. Similarly, Gene Mania (Figure 1), reports only two physical interactors: the Acyl-CoA Synthase ACSL6 and the zinc finger protein ZNF7 (Warde-Farley et al., 2010). All other interactions reported in this site are predicted or based on co-expression or computational analyses (Figure 1, blue, purple and orange lines).

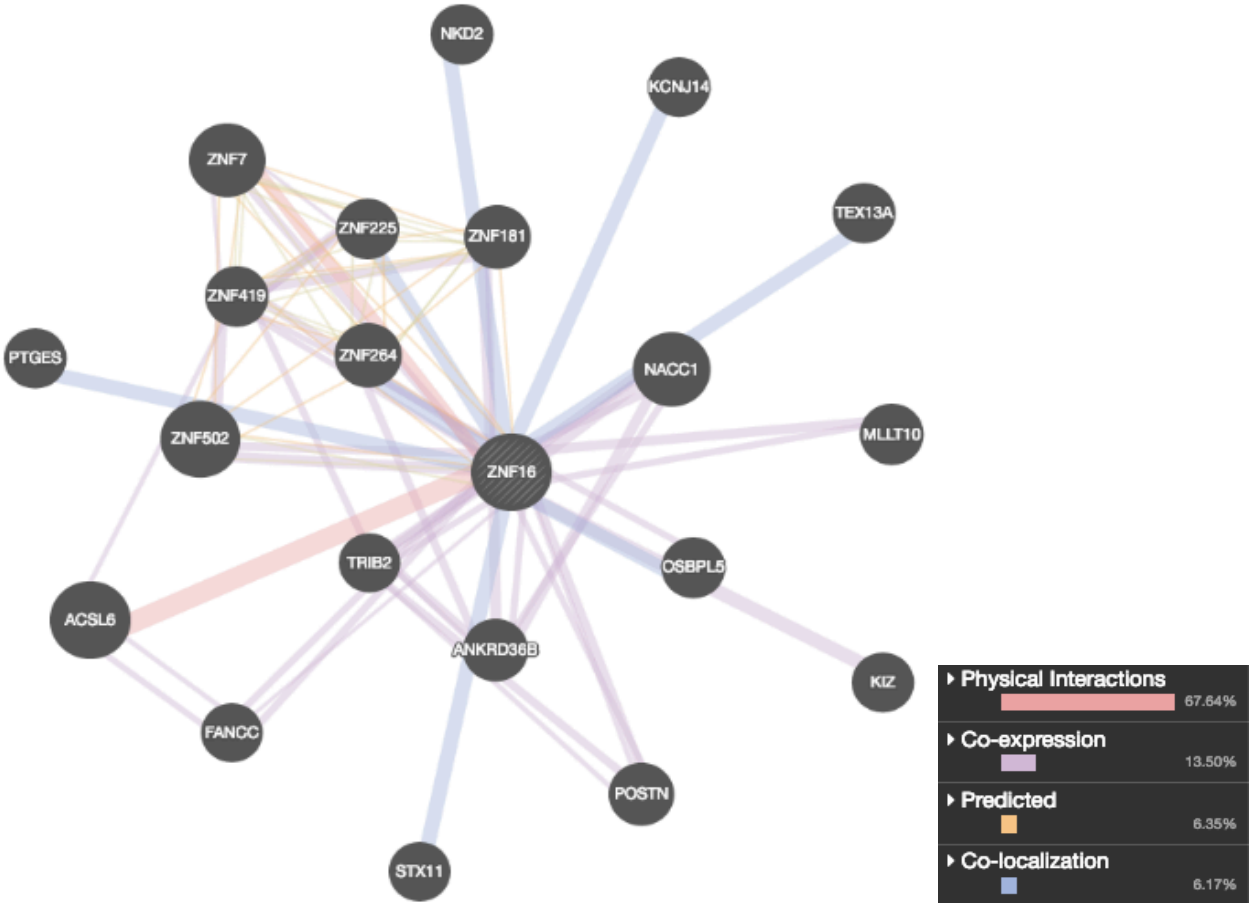


**Figure 1. Reported ZNF16 interactors.** Interaction map was obtained from GeneMania. Interactions are color coded by type as indicated in the figure legend.

*ZNF16 localization*

In the limited literature about ZNF16, there are reports of its nuclear localization. One such report demonstrated a nuclear localization of EGFP-tagged ZNF16 (Peng et al., 2006). Another report performed a serial deletion analysis to determine the amino acid residues that are responsible for the nuclear localization of ZNF16 and identified three nuclear localization signals within the zinc finger region of ZNF16 (Deng et al., 2009). However, none of these articles report the localization of endogenous ZNF16. The only information on this subject is found in the Cell Atlas, an open source database that includes immunofluorescence data for thousands of

proteins (Thul et al., 2017). Immunostaining images in this database indicate that ZNF16 has a more specific nucleolar localization.

*The nucleolus*

The nucleolus, one of the most visible internal compartments in the nucleus, is the site of rRNA synthesis, processing, and assembly of ribosomal subunits (Spector, 2001). Generally, a nucleus will contain several nucleoli of various size, depending on the cell type and level of transcriptional activity (Németh and Grummt, 2018). Cells with increased number and size of nucleoli have been reported in malignant tumor cells, serving to mark high energy demands of rapidly dividing cells and aid in aggressive tumor prognosis (Trinkle-Mulcahy, 2018). Diseases such as cancer, Alzheimers, and disorders of ribosome biogenesis, also known as ribosomopathies, have been connected with alterations to nucleolar morphology and function (Farley-Barnes et al., 2018). Deviations in morphology and function have also been observed in the ribosomal protein compositions in cells with viral infections (Hernandez-Verdun et al., 2010).

The nucleolus is a dynamic structure that contains over 800 proteins (Jarboui et al., 2011). From an architectural point of view, the nucleolus has three main structures: small Fibrillar Centers, associated with Dense Fibrillar Components, all surrounded by a Granular Component. The fibrillar center and its surrounding dense fibrillar component are the site of RNA synthesis (Reimer et al., 1987) and storage of newly transcribed pre-rRNA. The pre-rRNA is then thought to move to the granular component for further processing of the rRNAs and pre-ribosomal assembly (Shaw and Jordan, 1995). The rate at which the rDNA found in the

nucleolus is transcribed is highly efficient to support the metabolic activity of the cell and provide sufficient ribosomes (Grummt, 2003).

Because the nucleolus is not bound by a lipid membrane, it readily responds to cell stressors such as drug treatments, DNA damage, and viral infections, observed through changes in morphology and composition (Nicolas et al., 2016). Nucleolar structure and pre-rRNA synthesis are also dynamic throughout the cell cycle (Dousset et al., 2000; Klein and Grummt, 1999; Lamond and Earnshaw, 1998). Among the numerous proteins either permanently or temporarily residing in the nucleolus, many are cell cycle related proteins, and cell growth is negatively altered when ribosome production is impaired or limited (Pederson, 2011). Therefore the nucleolus can be an important cell stress sensor, disease biomarker, and target for cancer therapy (Nicolas et al., 2016).

The highly fluctuating nature of the nucleolus has been studied by analyzing the nucleolar proteome in natural and stress conditions such as drug induced transcriptional shutdown, UV and ionizing radiation, and adenovirus infection (Tafforeau et al., 2013). For example, upon exposure to inhibitors of RNA polymerase I, nucleolar integrity breaks down (Misteli, 2001), indicating that the integrity of the nucleolus requires continuous rRNA transcription. The inhibition of rRNA transcription leads to the delocalization of many nucleolar proteins, such as the RNA helicase II/Gu, from the nucleoli to the nucleoplasm (Scheer and Hock, 1999), thus providing clues about potential roles of these proteins related to rRNA synthesis (Rivera-León and Gerbi, 1997). Topoisomerase I, which is concentrated in the nucleoli, is another protein that delocalizes from the nucleoli to the nucleus. This delocalization occurs specifically in the presence of topoisomerase inhibitors, such as the anticancer drug, camptothecin (Mo et al., 2002).

Once cell stress, such as DNA damage, is sensed by the nucleoli, signals are transmitted from the nucleoli to the p53 pathway (Olson, 2004). Similarly, it has been shown that p53 activation can be promoted through specific inhibition of rDNA transcription in the nucleolus (Hein et al., 2013). In addition, cell stress can have a downregulation effect on rDNA transcription through the phosphorylation of the transcription factor, TIF-IA, blocking its normal interaction with RNA polymerase I (Mayer and Grummt, 2005). This suggests that nucleolar stress can lead to both reduction of rRNA and activation of p53, both of which can reduce cell proliferation. Consequently, RNA polymerase I inhibitors such as BMH-21 have been tested for anticancer activity in vitro (Peltonen et al., 2014) and small molecule inhibitors of RNA polymerase I have advanced to clinical trials (Quin et al., 2014) in hopes of curbing the nucleolar hijacking necessary for cancer cells to maintain high levels of protein synthesis and cell growth (Montanaro et al., 2008).

*ZNF16 function*

Reports of ZNF16 function are few and limited. There are suggestions that ZNF16 is a transcription factor based on nuclear localization, structural characteristics (Peng et al., 2006), and because the N-terminus of ZNF16 was observed to activate transcription of a lacZ reporter gene in yeast (Deng et al., 2009). Data collected from studies in chronic myelogenous leukemia (K562) cells points to a potential role for ZNF16 in erythroid and megakaryocytic differentiation (Peng et al., 2006). A related study found that ZNF16 acts as a transcriptional regulator of the c-KIT gene which is involved in erythroid and megakaryocytic differentiation (Chen et al., 2014).

Overexpression of ZNF16 in K652 cells suggests potential roles in apoptosis and the cell cycle. ZNF16 overexpression resulted in a slight increase in cell proliferation and the number of

cells in G2/M, and also slightly inhibited apoptosis triggered by sodium arsenate (Li et al., 2011). In zebrafish, a ZNF16-like protein is reported to regulate the specification of oligodendrocytes and is involved in migration and myelination in developing central nervous system (Sidik and Talbot, 2015). While these phenotypes indicate that ZNF16 might have multiple functions, the molecular mechanisms for ZNF16 function are unknown.

*Localization and roles of other zinc finger proteins*

Since there is little information about ZNF16 function, we also explored other zinc finger proteins with similar characteristics to identify potential functions for ZNF16. We particularly focused on those localized in the nucleoli. ZNF274, is a ubiquitously expressed transcription repressor, localized in the nucleoli (Yano et al., 2000), but its function is similarly unknown. ZPR1, which interacts with the cytoplasmic domain of receptor tyrosine kinases, accumulates in the nucleolus of proliferating cells. Depletion of ZRP1 through a gene disruption strategy causes disruption in nucleolar function, specifically in preribosomal RNA expression (Galcheva-Gargova et al., 1998). In a study exploring the effects of depleted levels of Pf1, a transcriptional modulator in mouse embryonic fibroblasts, impaired proliferation and an increase in senescence-associated β-galactosidase activity were reported. Findings showed elevated levels of DNA double-stranded breaks and a strong activation of the DNA damage response. The report also shows Pf1 has a role in multiple regulation steps of the ribosome biogenesis pathways and in nucleolar morphology, as well as interactions with proteins involved in ribosome biogenesis (Graveline et al., 2017).

Overexpression of PAG608, a p53 inducible gene, demonstrated nucleolar localization, alterations in nucleolar structure, and promoted apoptosis (Israeli et al., 1997). Similar to

PAG608 is ZNF545/ZFP82, another nucleolar zinc finger protein, which showed tumor cell growth suppression characteristics and was found to be frequently silenced in several carcinomas (Cheng et al., 2012) and in several gastric cancer cell lines (Wang et al., 2013). LYAR, localizes in the nucleoli, is involved in rRNA processing (Miyazawa et al., 2014) and has been reported to play a role regulating cell growth (Su et al., 1993; Sun et al., 2017). Finally, PARP-1, a nucleolar protein, delocalizes from the nucleoli to the nucleoplasm in cells exposed to DNA damage where it is involved in the DNA repair system, binding directly to DNA breaks (Rancourt and Satoh, 2009). Based on these findings, zinc finger proteins with nucleolar localizations, seem to have roles in cell proliferation, DNA repair, and ribosomal biogenesis.

# CHAPTER 2: RESEARCH GOAL AND SPECIFIC AIMS

**Research Goal:** The overall goal of this research is to determine the function of the human ZNF16 protein at the cellular and molecular level.

Based on the limited information about ZNF16 and on research pertaining to related zinc-finger proteins, I hypothesize that ZNF16 has roles in DNA damage and nucleolar functions such as rRNA synthesis. To test these hypotheses, I will analyze the role of ZNF16 through the following aims:

**Specific Aim 1:** Assess if ZNF16 plays a role in DNA repair. This aim seeks to survey if changes in ZNF16 expression induce DNA damage or alter the response to DNA damage.

**Specific Aim 2:** Examine if ZNF16 is involved in nucleolar structure or rRNA synthesis. First, we will confirm the reported nucleolar localization of ZNF16, followed by the determination of possible phenotypes resulting from overexpression of ZNF16 on nucleolar structure or function.

# CHAPTER 3: MATERIALS AND METHODS

## Cell Culture

HeLa Tet-On, U2OS mCherry-mito, DLD1, RPE1, and Hct116 cells were grown in a humidified incubator at 37°C with 5% $CO_2$ in Dulbeccos modified Eagles medium (DMEM; Corning) supplemented with 10% fetal bovine serum (FBS; HyClone) and 2mM GlutaMAX -I (100X) (Life Technologies).

## Plasmids and siRNAs

Plasmid used in this study include: pIRESpuro-EGFP (EGFP), pIRESpuro-EGFP-ZNF16 (EGFP-ZNF16), pIRESpuro-3xEGFP-ZNF16 (3xEGFP-ZNF16) kindly provided by Laura Diaz-Martinez. Both ZNF16 plasmids include the 3'UTR of ZNF16 and have silent mutations that make them resistant to siRNAs. pHrD-IRES-Luc (human rRNA promoter-luciferase reporter) (kindly provided by K. Ghoshal) and pIRES-Luciferase (kindly provided by Z. Karamysheva). Endogenous siRNA knockdown was performed using siZNF16-E, 5'-AAACUAUGCUGGUGAUGUU-3' (Dharmacon).

## Plasmid Transfection

Plasmid transfections were performed using Lipofectamine 2000 (Life Technologies) for Hela Tet-On cells and U2OS mCherry-mito cells. Cells were plated and transfected simultaneously. Transfections were preformed following the manufacturer recommendations with the following modifications: 8-well chambered slide (250 μL total volume:0.56 μL Lipofectamine 2000:100ng plasmid), 96-well plate (130 μL total volume:0.336 μL Lipofectamine 2000:60ng plasmid).

## siRNA Transfection

Cells were plated and transfected simultaneously and untransfected cells were used as controls. siRNA transfections were completed using Lipofectamine RNAiMAX according to the

manufacturer recommendations with the following modifications: 8-well chambered slide (250 μL total volume:0.25 μL Lipo RNAiMAX), 96-well plate (130 μL total volume:0.15 μL Lipo RNAiMAX), 6-well plate (2mL total volume:2.5 μL Lipo RNAiMAX), with 25nM of siRNA.

**Western Blot**

Cells were washed in PBS and lysed in lysis buffer (250mM SDS, 82.5mM Tris Base, 30% glycerol, 1.5mM bromophenol blue, and 43.7mM DTT), sonicated, and boiled for 10 minutes. Samples were separated by SDS-PAGE and transferred to a nitrocellulose membrane (GE Healthcare Life Sciences) using a semi-dry transfer apparatus (BioRad). The membranes were incubated with primary antibodies against ZNF16 (Rabbit anti-ZNF16 at 1:50; Sigma-Aldrich), GFP (Rabbit anti-GFP at 1:500; Novus), and/or tubulin (Mouse anti-tubulin ascites at 1:100; kindly provided by Dr. Roychowdhury) dissolved in 5% non-fat dry milk in TBS-T (1X TBS + 0.01% Tween) overnight at 4°C. Secondary antibodies (Promega Anti-Rabbit IgG HRP Conjugate and Anti-Mouse IgG HRP Conjugate at 1:2000) and the membrane were incubated at room temperature for 30 minutes. Proteins were visualized using enhanced chemiluminescence reagents (SuperSignal West Pico Chemiluminescent Substrate; Pierce) and detected by iBright FL1000 Imaging System (Thermo Fisher).

**Immunostaining**

After cells were transfected and cultured for 24 hours in 8 well chamber slides (Nunc Lab-Tek) cells were fixed with 4% paraformaldehyde for 20 minutes at room temperature. Primary antibodies against ZNF16 (Rabbit anti-ZNF16 at 1:50; Sigma-Aldrich), GFP (Rabbit anti-GFP at 1:500; Novus), Ki67 (Mouse anti-Ki67 at 1:250; BD Biosciences), and the DNA damage marker γH2AX (Mouse anti-γH2AX at 1:200; BD Biosciences) were diluted in blocking buffer (0.2% Triton X-100 in PBS with 3% BSA) and incubated at 4°C overnight. Secondary antibodies

(Alexa Fluor 488 donkey anti-rabbit IgG (H+L) and Alexa Fluor 568 donkey anti-mouse IgG (H+L); Invitrogen by Thermo Fisher Scientific) were diluted in blocking buffer and incubated at room temperature, in the dark for 30 minutes. High-resolution digital fluorescent images from HeLa and U2OS cells, stained with DAPI, were captured by using an LSM 700 confocal microscope (Zeiss, New York, New York, USA), equipped with an EC Plan-NEOFLUAR 63x/1.25 oil immersion objective and ZEN 2009 software (Zeiss), for acquisition and processing of the confocal images. Multi-plane images were sequentially scanned using a 1-Airy unit pinhole setting and a 405 nm laser. Images were processed using ImageJ.

**rDNA Luciferase Assay**

Cells were transfected with either plasmid pHrD-IRES-Luc (human rRNA promoter-luciferase reporter) (kindly provided by K. Ghoshal) or plasmid pIRES-Luciferase (minimal CMV promoter) (kindly provided by Z. Karamysheva). After forty-eight hours, luminescence was measured with ONE-Glo Luciferase Assay System and detected with a Labsystems Luminoskan Ascent plate reader at room temperature. The results of five assays were statistically analyzed in excel.

**qPCR Assay**

RNA was extracted from cells using TRIzol and Isopropanol precipitation. RNA extracts were subjected to qPCR using the Applied Biosystems Power SYBR Green RNA-to-$C_T$ 1-Step Kit, according the manufacturers instructions in an Applied Biosystems Step One Plus Real-Time PCR System. The qPCR assays were completed in technical and biological triplicates. The primers used for qPCR were: (pre-rRNA-forward: GCCTTCTCTAGCGATCTGAGAG, pre-rRNA-reverse: CCATAACGGAGGCAGAGACA, GAPDH-forward: GGTGGTCTCCTCTGACTTC, GAPDH-reverse: CTCTTCCTCTTGTGCTCTTG, ZNF16-

forward: GCCTTCAACCGAAGCTCAAAT, ZNF16-reverse:

GGATGAGGACCGAACGCTG).

**Actinomycin D Treatments**

To visualize effects of the inhibition of RNA Polymerase I, cells were treated with 40 μM Actinomycin D for four hours. Vehicle (DMSO) was used as control.

**DNA damage Treatments**

To visualize the effects of DNA damage, cells were treated with 20 μM cisplatin,10 μM Camptothecin or DMSO (control) for four hours. Irradiation of cells was carried out with a dose of 5Gy by use of a X-RAD 160 (Precision X-Ray Inc. N. Brandford, CT USA).

# CHAPTER 4: RESULTS

ZNF16 is an understudied gene that has been implicated in blood cell differentiation (Peng et al., 2006) and cell proliferation related processes (Díaz-Martínez et al., 2014; Li et al., 2011). However, the research on its function is limited. Based on the localization of ZNF16 in the nucleus or nucleolus (Deng et al., 2009; Thul et al., 2017), it is possible ZNF16 could have a role in nucleolar structure, ribosome synthesis and processing, or the DNA damage response. This research looks to identify a potential role of ZNF16 at the cellular and molecular level.

Founded on the limited information about ZNF16 function, ubiquitous ZNF16 expression, and research pertaining to related zinc-finger proteins, I hypothesized that ZNF16 has multiple roles, including roles in the response to DNA damage and nucleolar functions such as rRNA synthesis.

## *ZNF16 is expressed in a wide range of cell lines*

Before we began testing for ZNF16s localization and potential functions, we analyzed expression levels of ZNF16 in various cell lines (Figure 2) to test whether ZNF16 is expressed in different cell lines and guide our choice in cell lines to use in the upcoming experiments. We tested for ZNF16 expression in four cancer cell lines (HeLa, U2OS, DLD1, Hct116) and one non-cancer cell line (RPE1, immortalized epithelial cells). ZNF16 mRNA was detected in all cell lines tested with the lowest expression being observed in HeLa cells, while U2OS had the highest expression, 30-fold higher than HeLa (Figure 2). These two lines were selected for subsequent experiments based on the idea that overexpression assays would perhaps have a more dramatic effect in HeLa cells while U2OS cells might experience greater effects from future knockdown assays.

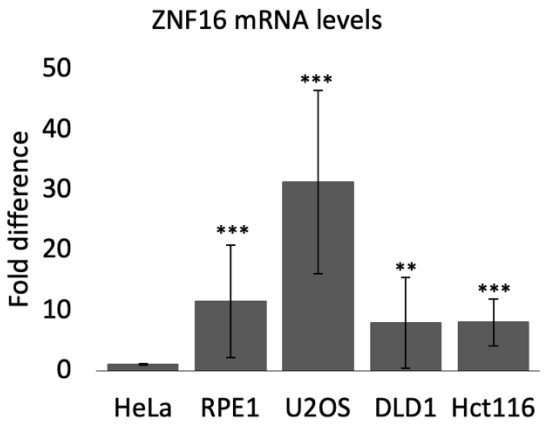


**Figure 2. ZNF16 mRNA levels in various cell lines.** Cells were cultured for 48 hours and mRNA levels were measured via qPCR. The graphs represent the mean and standard deviation from 3 independent assays. (*** $p<0.001$)

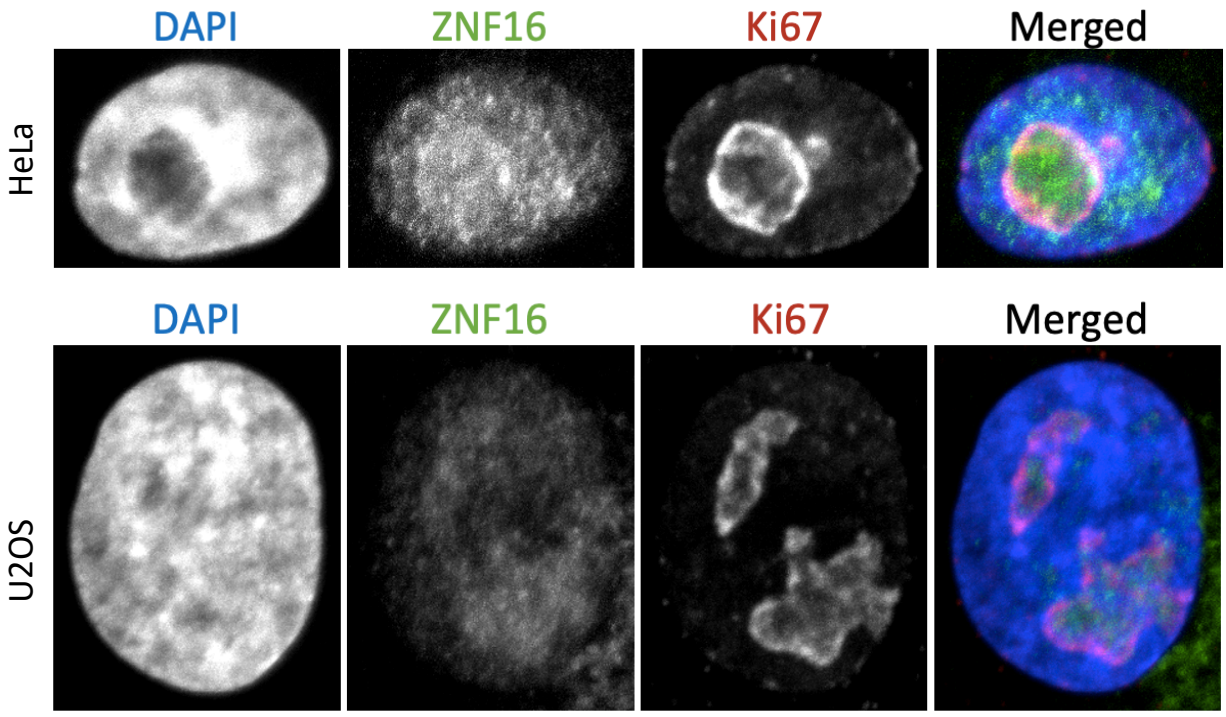


**Figure 3. Localization of endogenous ZNF16 in HeLa and U2OS cells.** HeLa TetON and U2OS cells were fixed and immunostained with antibodies against ZNF16 and the nucleolar marker Ki67 and visualized by confocal microscopy.

*Endogenous ZNF16 localizes to the nucleus and is enriched in the nucleoli*

To elucidate the localization of ZNF16, endogenous ZNF16 was visualized in both HeLa and U2OS cells through immunofluorescence, staining for DAPI, ZNF16, and Ki67, a protein known to localize to the nucleoli (Verheijen et al., 1989). Endogenous ZNF16 localized in the nucleus, counterstained with DAPI, and appeared to be enriched in the nucleoli (Figure 3), indicating that endogenous untagged ZNF16 localizes both in the nucleus and nucleolus in both cell lines. To quantify this potential enrichment, we used ImageJ to determine ZNF16 levels in the nucleus and the nucleolus. We began by defining the boundaries of the nucleus and nucleoli by drawing a line through the cell stained for the nucleolar marker Ki67. To do this, we ran a plot profile of the line through the cell stained for Ki67 which reports the quantified amount of signal across each point of the line and therefore set the boundaries of the nucleoli, through the nucleolar marker (Figure 4). We then repeated this process for ZNF16, obtaining the plot profile of signal across the nucleus and applied the nucleolar boundaries, obtained from Ki67, to the plot profile for ZNF16 to separate ZNF16 signal points in the nucleus from those in the nucleoli (Figure 4A and B).

Data points belonging in the nucleus and nucleoli were then normalized to a baseline (average of the lowest 50 signal values) to obtain a fold difference over baseline value for each point. Normalizing the data from each cell to its baseline allows us to account for the natural variation in signal levels between individual cells. Using the normalized data points, we took the average of the points within the nucleolar boundaries and compared them to the average of the nuclear points. The graphs (Figure 5) show there is a higher average signal of Ki67 in the nucleoli than in the nucleus, which we expected as Ki67 is a reported nucleolar protein. We also observe a higher average signal of ZNF16 in the nucleoli compared to the nucleus in both cell

types. This both confirms an enrichment of ZNF16 in the nucleoli and suggests ZNF16 may reside in multiple locations and perhaps have multiple roles.

A caveat of this experiment is that the ZNF16 signal was very weak, even when we used the antibody at high concentrations. To corroborate these results, we next performed similar experiments to test the localization of exogenous ZNF16.

*Exogenous ZNF16 localizes to the nucleus and nucleoli in a tag-dependent manner*

For exogenous ZNF16 localization we transfected EGFP-ZNF16 and 3xEGFP-ZNF16 plasmids in HeLa and U2OS cells. An EGFP plasmid was transfected as control. Samples were then immunostained for EGFP to mark the exogenous ZNF16 and Ki67 to mark the nucleoli. Interestingly, HeLa cells transfected with EGFP-ZNF16 showed ZNF16 localizing in the nucleus, consistent with prior reports (Deng et al., 2009; Peng et al., 2006), while those transfected with 3xEGFP-ZNF16 demonstrated ZNF16 colocalizing with Ki67 in the nucleoli (Figure 6). It was also observed that exogenous 3xEGFP-ZNF16 produced two localization patterns, with 65% of cells showing ZNF16 solely in the nucleoli, while 35% of cells contained ZNF16 in the nucleoli and in subnuclear structures in a freckled distribution.

In U2OS cells we observed similar localization patterns with a few differences (Figure 6). The ZNF16 tagged with one EGFP localized to the nucleus like HeLa cells but is also seen in the nucleoli. In HeLa cells we saw ZNF16 tagged with triplicate EGFP in the nucleoli and sometimes subnuclear structures but in U2OS cells we observed triplicate EGFP tagged ZNF16 solely in the nucleoli. As with endogenous ZNF16, we quantified the presence of EGFP tagged ZNF16 and 3xEGFP tagged ZNF16 in the nucleoli and our results confirm our observations of

EGFP-ZNF16 being enriched in the nucleoli in U2OS cells and 3xEGFP-ZNF16 being enriched in the nucleoli in both cell lines (Figure 7).

These results suggest the interesting hypothesis that ZNF16 localizes to both the nucleus and the nucleolus, and that the tags used in the exogenously expressed ZNF16 experiments favor one localization over the other, with EGFP-ZNF16 localizing the nucleus and avoiding the nucleoli in HeLa cells while localizing in both the nucleus and nucleoli in U2OS cells. The data also indicate 3xEGFP-ZNF16 accumulates mainly in the nucleoli in both cell lines. A potential explanation is that the tags might differentially interfere with the binding of ZNF16 to proteins in the nucleus or the nucleolus, suggesting that different domains might be involved in the two patterns of localization. Importantly, the differential localization of exogenous ZNF16 can be used as a tool to allow us to interrogate the specific role of ZNF16 at these two locations independently. No major changes were observed in nucleolar morphology in cells expressing exogenous ZNF16. However, a more detailed analysis is warranted to analyze whether ZNF16 overexpression causes changes in the nucleolus.

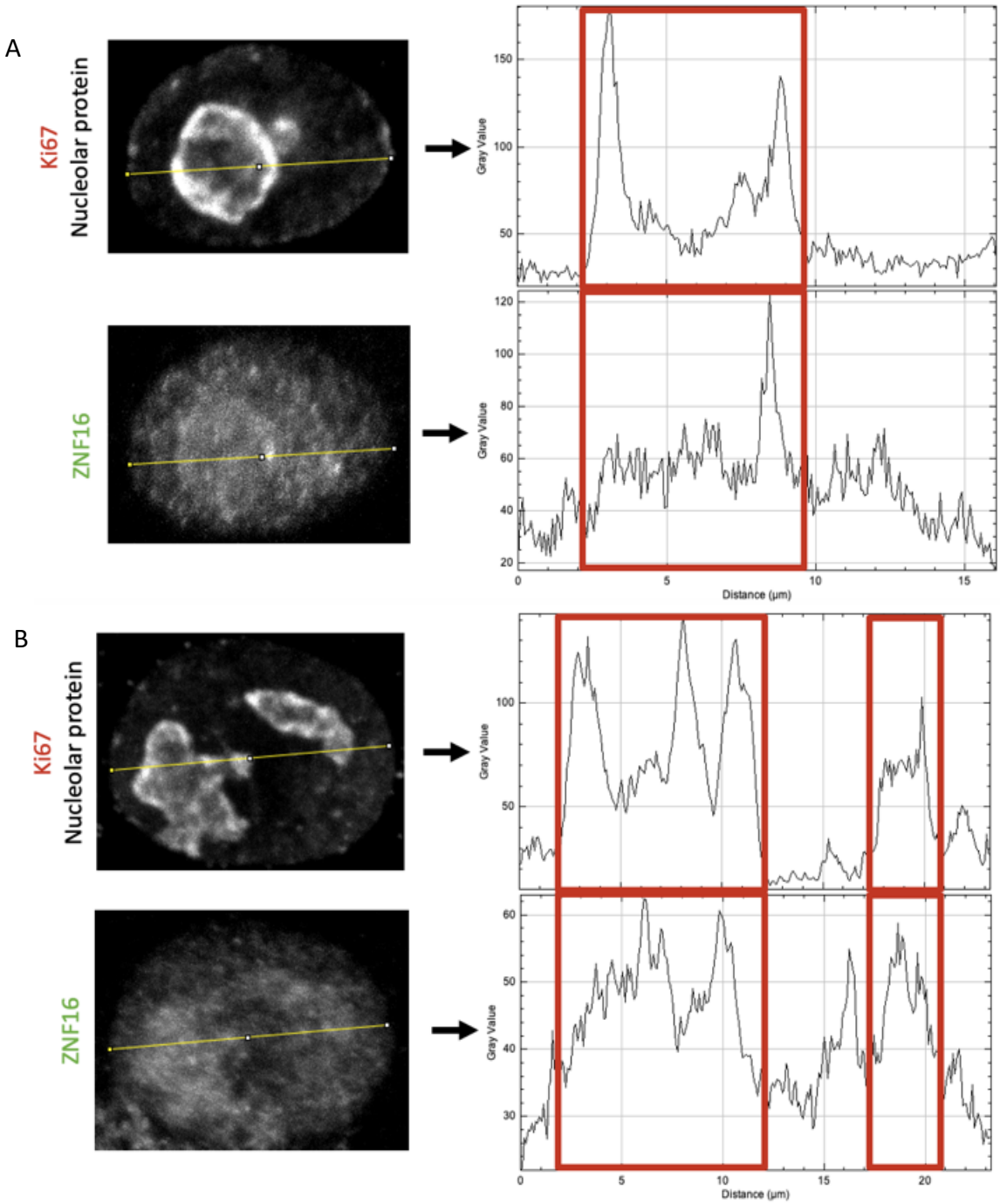


**Figure 4. Endogenous ZNF16 enriched in the nucleoli.** Cells were fixed and immunostained with antibodies against ZNF16 and the nucleolar marker Ki67 and visualized by confocal microscopy. Image J was then used to draw a line through each cell resulting in signal points across the line. Nucleolar boundaries were set using the nucleolar marker Ki67 (A and B). Data points belonging in the nucleus and nucleoli were then analyzed by creating a baseline from the average of the lowest 50 signal values. Each raw data point was normalized to the respective baseline to calculate a fold difference over baseline value. Using the normalized data points, the average of the points within the nucleolar boundaries (marked by the red rectangles) were compared to the average of the nuclear points for Hela (A) and U2OS (B) cells (n=30, 10 cells from 3 trials).

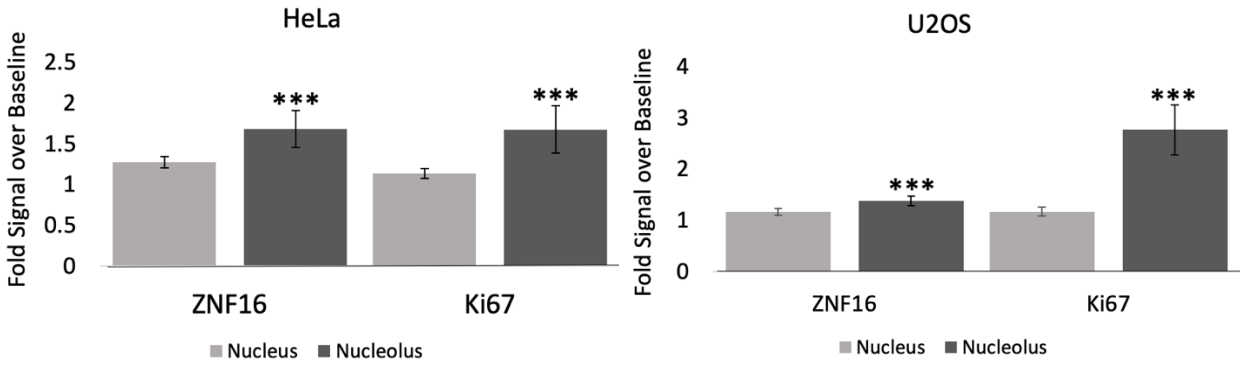


**Figure 5. Endogenous ZNF16 enriched in the nucleoli.** Comparison of signal intensity for ZNF16 and Ki67 in the nucleus and nucleoli of HeLa and U2OS cells quantified as described in Figure 4. Graphs show the average ± standard deviation of 30 cells from 3 independent trials (n=30, 10 cells from 3 trials). (*** $p<0.001$)

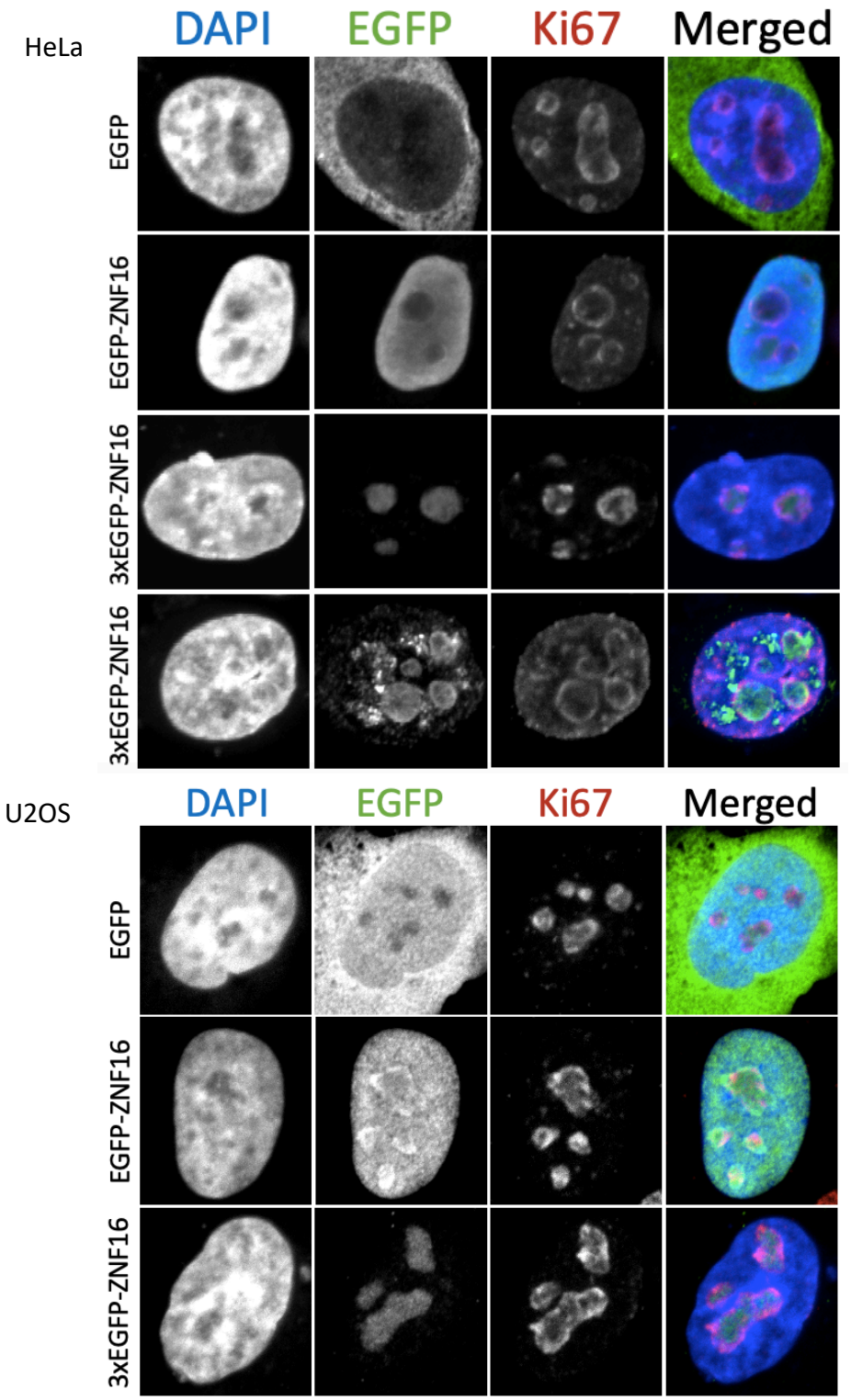


**Figure 6. Exogenous ZNF16 shows different patterns of localization.** HeLa and U2OS cells were transiently transfected with the indicated plasmids. The cells were fixed twenty-four hours after transfection and immunostained with antibodies against EGFP and the nucleolar marker Ki67 and visualized by confocal microscopy.

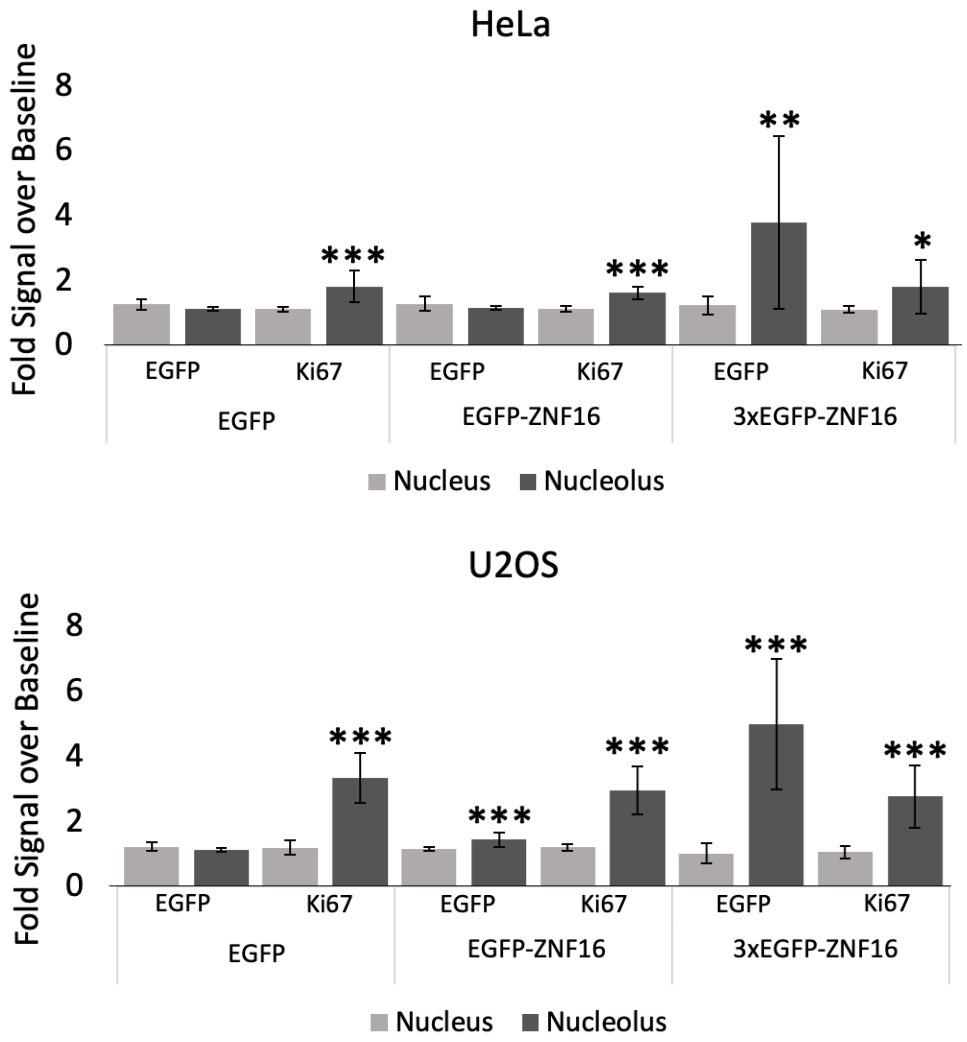


**Figure 7. Exogenous ZNF16 enriched in the nucleoli**. Hela and U2OS cells were cultured for 24 hours with the transfected plasmids and were then fixed and immunostained with antibodies against GFP and the nucleolar marker Ki67 and visualized by confocal microscopy. Image J was then used to obtain line plots for each cell (n=30, 10 cells from 3 trials). Nucleolar boundaries were set using the nucleolar marker Ki67. Data point belonging in the nucleus and nucleoli were then analyzed by creating a baseline from the average of the lowest 50 signal values. Each raw data point was normalized to the respective baseline to have a fold difference over baseline value. Using the normalized data points, the average of the points within the nucleolar boundaries were compared to the average of the nuclear points. (*** $p<0.001$)

*Specific Aim 1: Assess if ZNF16 plays a role in DNA repair*

Following reports of increased DNA damage in cells with depleted levels of Pf1, a zinc finger protein (Graveline et al., 2017), and sensitivity of the nucleolus to cell stressors such as DNA damage, which result in changes in nucleolar morphology or composition (Nicolas et al., 2016). We wanted to see if expression levels of ZNF16 resulted in DNA damage or changes in the response to DNA damage.

There are numerous ways DNA can become damaged, therefore cells must have mechanisms to respond (Friedberg, 2003). Cells need to be able to detect the damage, signal the presence of damage, and then mediate the repair of the damaged DNA (Jackson and Bartek, 2009). Damage to the chromosomes results in the activation of complex response pathways and DNA repair networks (Zhou and Elledge, 2000), and if the damage cannot be repaired, programed cell death processes are activated (Sancar et al., 2004). Response reactions include the removal and repair of the damaged DNA via numerous repair mechanisms, arresting the cell cycle progression through the activation of DNA damage checkpoints, changes in the transcriptional response that maybe beneficial to the cell, and activation of the apoptotic pathway.

Crosstalk between the DNA repair response and the nucleolus have been documented. For example, the Nucleotide Excision Repair (NER) protein, TFIIH, moves freely between the NER complex and the RNA polymerase I complex. This shared protein, as well as others, suggest a close interrelationship between DNA repair and rRNA synthesis (Grummt, 2003).

*Overexpression of ZNF16 results in cell line-dependent changes in DNA damage*

First, we tested whether overexpression of ZNF16 induced DNA damage in the absence of any DNA damaging agents. HeLa and U2OS cells were each transiently transfected with EGFP-ZNF16, 3xEGFP-ZNF16 and EGFP (control). The cells were then fixed and immunostained for GFP to visualize ZNF16 expression and with γH2AX, a marker of DNA damage (Mischo et al., 2005). Cells were imaged via confocal microscopy and analyzed using ImageJ. To account for variations in nuclei size, gH2AX signal was normalized to the DAPI signal in the same cell.

HeLa cells transfected with 3xEGFP-ZNF16, which localizes to the nucleoli, show a slight increase in DNA damage compared with cells transfected with the EGFP control (Figures 8 and 9), while EGFP-ZNF16 overexpression does not result in changes in DNA damage. However, U2OS cells transfected with either EGFP-ZNF16, localizing primarily to the nucleus, or 3xEGFP-ZNF16, localizing to the nucleoli, show a decrease in DNA damage compared to the EGFP control (Figures 8 and 9). Essentially, the overexpression of ZNF16 increasing DNA damage in one cell line, while decreasing DNA damage in another cell line, implies that the effect of ZNF16 overexpression is not conserved and thus does not suggest a universal role for ZNF16 in this process.

Next, we tested whether ZNF16 was involved in the response to DNA damage through the employment of several DNA damaging agents. After transfection with the plasmids indicated above, cells were treated with the following DNA damaging agents: 20 μM cisplatin for four fours (Roos and Kaina, 2006), 10 μM camptothecin for four hours, or a 5Gy dose of x-ray radiation to induce DNA damage. These DNA damage agents were selected as representatives of the different types of DNA damage cells can encounter, cisplatin causes adducts, camptothecin

results in single strand breaks and x-rays produces double strand breaks (De Bont and van Larebeke, 2004). This allows us to comprehensively test the potential involvement of ZNF16 in the response to different types of DNA damage.

Cisplatin, commonly used as an anticancer drug to treat solid tumors, binds to DNA forming adducts and interferes with replication and transcription (Basu and Krishnamurthy, 2010). When HeLa cells overexpressing ZNF16 were treated with cisplatin, we observed an increase in DNA damage compared to EGFP control cells (Figures 10 and 11), with nucleolar ZNF16 (3xEGFP-ZNF16) having the most significant effect. Interestingly we observe the opposite trend in U2OS cells with cells overexpressing ZNF16 in the nucleoli (3xEGFP-ZNF16) showing a decrease in DNA damage (Figures 10 and 11). These results indicate that the effects of ZNF16 overexpression on cisplatin-induced DNA damage are cell type specific.

The next DNA damaging agent tested, camptothecin, inhibits topoisomerase I leading to single-stranded breaks, and after replication, lethal double-stranded breaks (Mo et al., 2002). In HeLa cells treated with camptothecin, there is an increase in DNA damage when ZNF16 is overexpressed in the nucleus and a decrease in DNA damage when ZNF16 is overexpressed in the nucleoli (Figures 12 and 13). A decrease in DNA damage was also observed in camptothecin-treated U2OS cells with an overexpression of ZNF16 in the nucleoli (Figures 12 and 13). The significant decrease in camptothecin-induced DNA damage observed in both HeLa and U2OS cells when ZNF16 is overexpressed in the nucleoli is especially intriguing because camptothecin inhibits topoisomerase I, which is enriched in the nucleoli (Mo et al., 2002). These results suggest that nucleolar ZNF16 might be protective against damage caused by inhibition of nucleolar proteins.

The final DNA damaging agent employed was x-ray irradiation, which causes DNA double-strand breaks (Snyder and Lachmann, 1989). HeLa cells with an overexpression of ZNF16 in the nucleoli showed a decrease in DNA damage when exposed to x-rays and compared to EGFP controls (Figures 14 and 15) while nuclear ZNF16 did not have an effect. The results were the reverse in U2OS cells, with ZNF16 overexpression in the nucleus of U2OS cells resulting in an increase in DNA damage after x-ray treatment, compared to controls (Figures 14 and 15). The observations from these data suggest that the effects of ZNF16 overexpression on x-ray induced DNA damage are cell line specific.

Overall there does not appear to be a consistent trend in the relationship between ZNF16 overexpression and DNA damage (Figure 16), with one notable exception. While there is no clear relationship between ZNF16 levels or localization and the response to cisplatin or x-rays, it is very intriguing that ZNF16 overexpression in the nucleoli, via 3xEGFP-ZNF16 plasmid transfection, showed significant decreases in DNA damage in the presence of camptothecin in both cell lines tested. Intriguingly, camptothecin is a Topoisomerase I inhibitor and Topoisomerase I is enriched at the nucleolus (Mo et al., 2002). It will be interesting to test more cell lines to see if the protection against camptothecin is conserved. In summation, the lack of conserved phenotypes across DNA damaging agents and cell lines essentially leads to the conclusion that there is not a universal role for ZNF16 in the DNA damage process, but the decrease of camptothecin-induced damage when nucleolar exogenous ZNF16 is expressed, suggests a role for ZNF16 in nucleolar-related DNA damage.

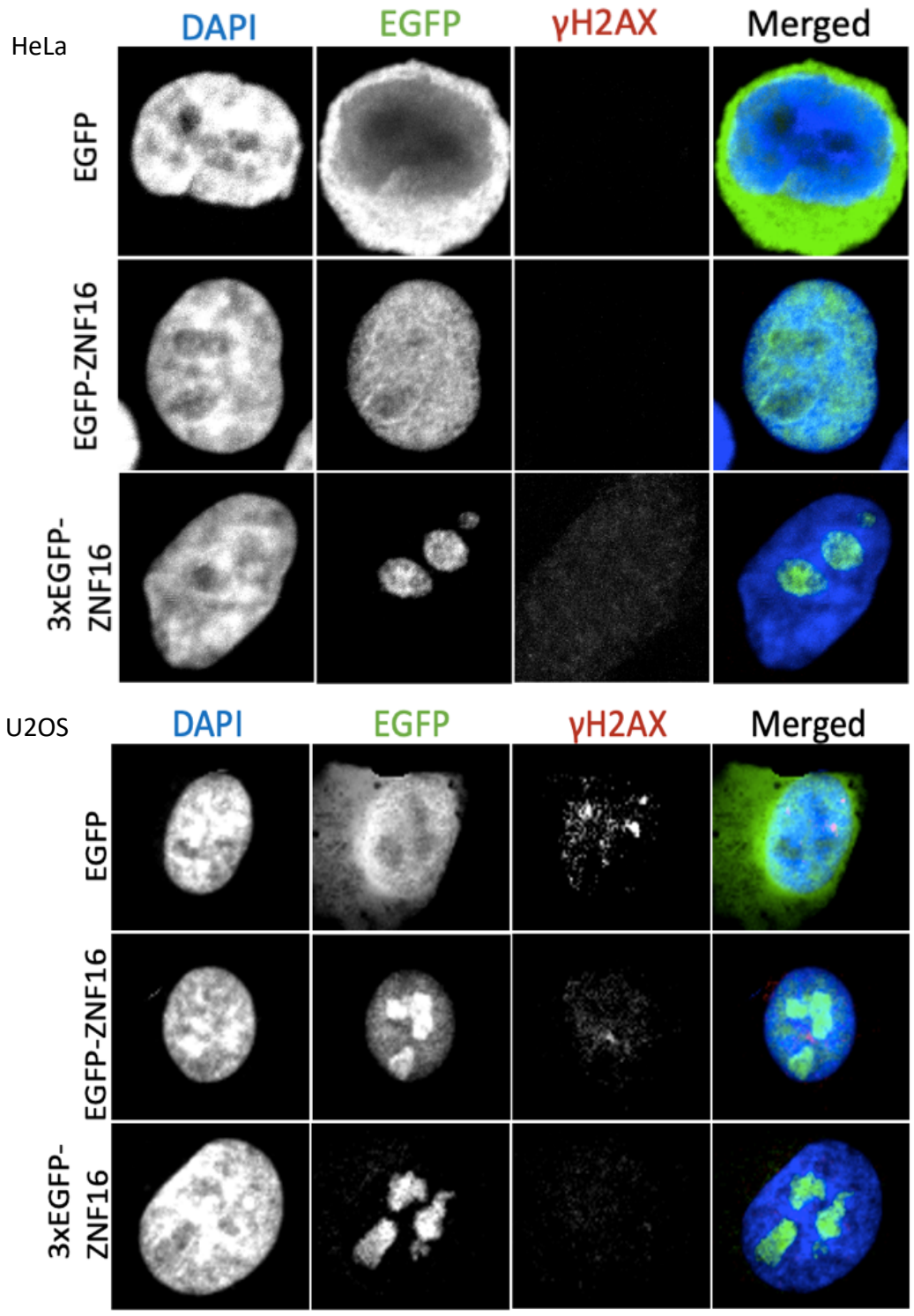


**Figure 8. Effect of ZNF16 overexpression on the DNA damage response of untreated HeLa and U2OS cells.** HeLa and U2OS cells were transiently transfected with the indicated plasmids. Before fixation, cells were treated with DMSO. The cells were fixed twenty-four hours after transfection and immunostained with antibodies against EGFP and the DNA damage marker γH2AX. Cells were then visualized by confocal microscopy.

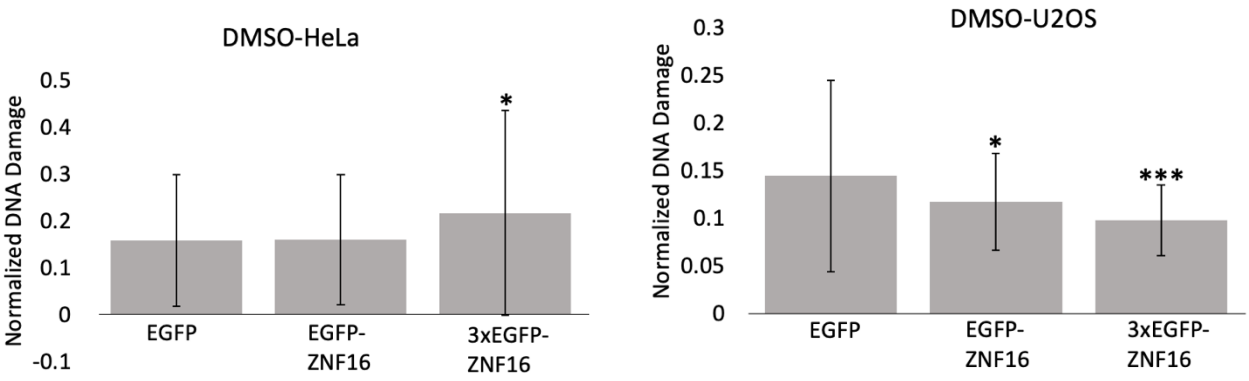


**Figure 9. Effect of ZNF16 overexpression on the DNA damage response of untreated HeLa and U2OS cells.** Quantification of gH2AX intensity after transfection with exogenous ZNF16. gH2AX intensity was quantified in immunofluorescence images obtained as described in Figure X using ImageJ. Briefly, DAPI signal was used to delineate the nucleus of each cell and intensity of gH2AX was measured per nucleus and normalized to DAPI. (n=30, 10 cells from 3 trials) (* p.0.5, *** $p<0.001$)

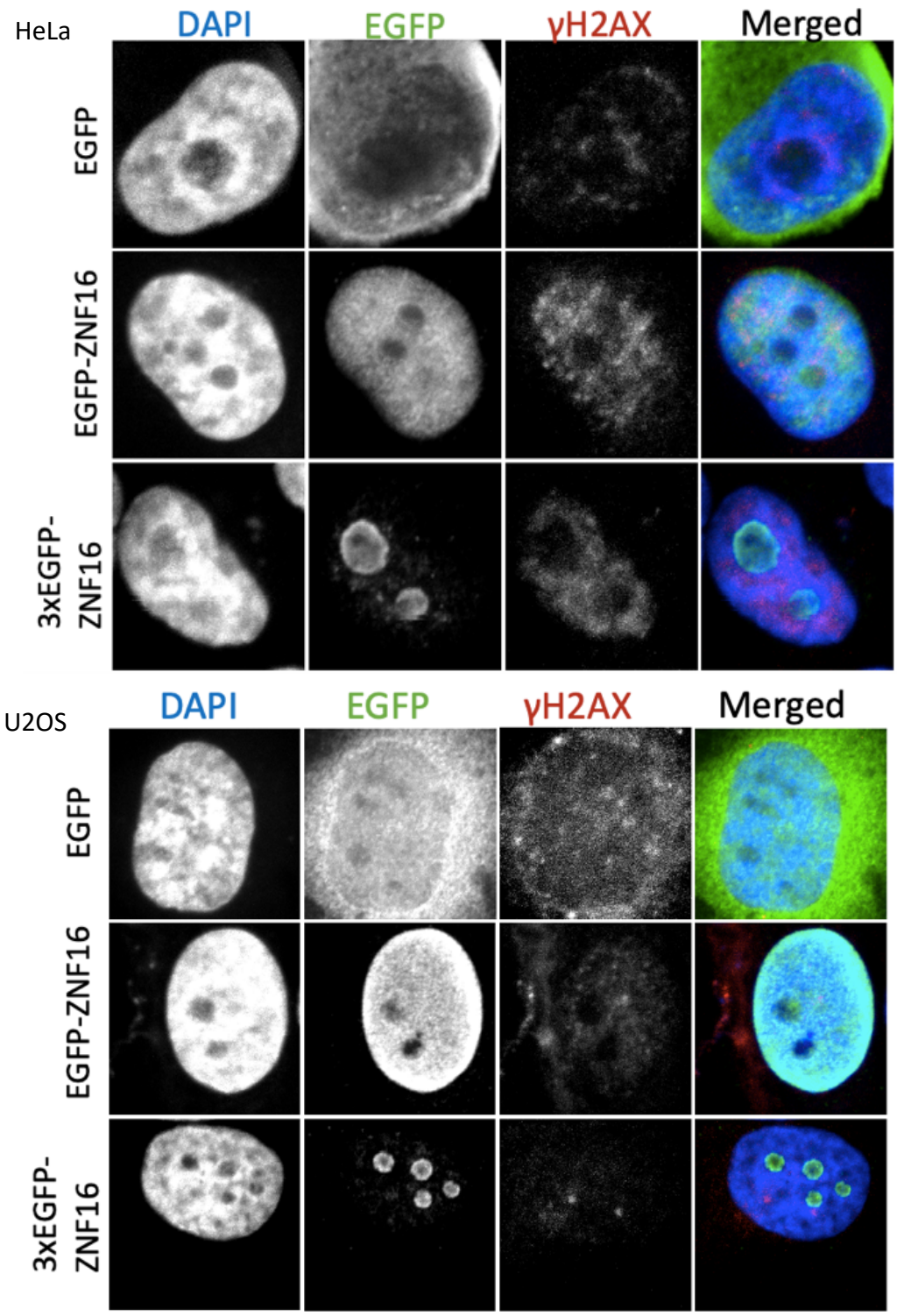


**Figure 10. Effect of ZNF16 overexpression on the DNA damage response of HeLa and U2OS cells treated with cisplatin.** HeLa TetON and U2OS cells were transiently transfected with the indicated plasmids. Before fixation, cells were treated with 20 μM cisplatin for four hours. The cells were fixed twenty-four hours after transfection and immunostained with antibodies against EGFP and the DNA damage marker γH2AX. Cells were then visualized by confocal microscopy.

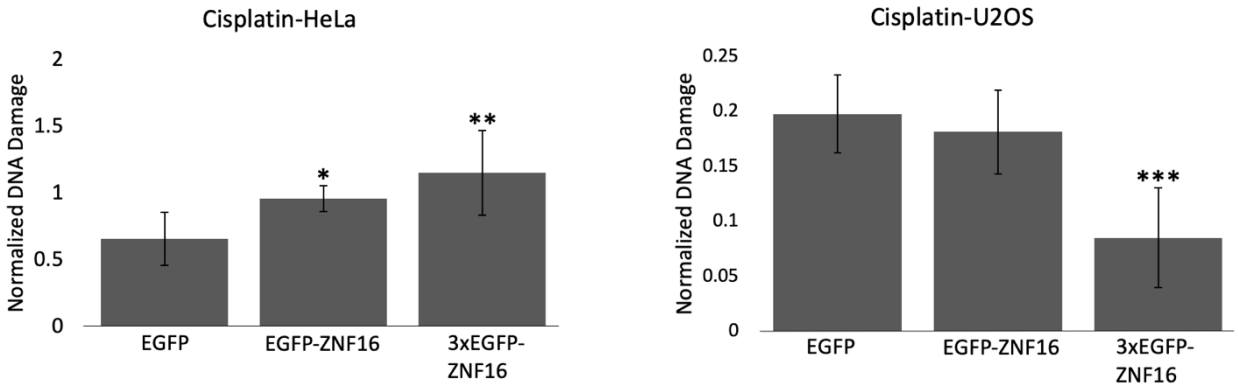


**Figure 11. Effect of ZNF16 overexpression on the DNA damage response of HeLa and U2OS cells treated with cisplatin.** Quantification of gH2AX intensity after transfection with exogenous ZNF16. gH2AX intensity was quantified in immunofluorescence images obtained as described in Figure X using ImageJ. Briefly, DAPI signal was used to delineate the nucleus of each cell and intensity of gH2AX was measured per nucleus and normalized to DAPI. (n=30, 10 cells from 3 trials) (*$p<0.5$, **$p<0.01$, *** $p<0.001$)

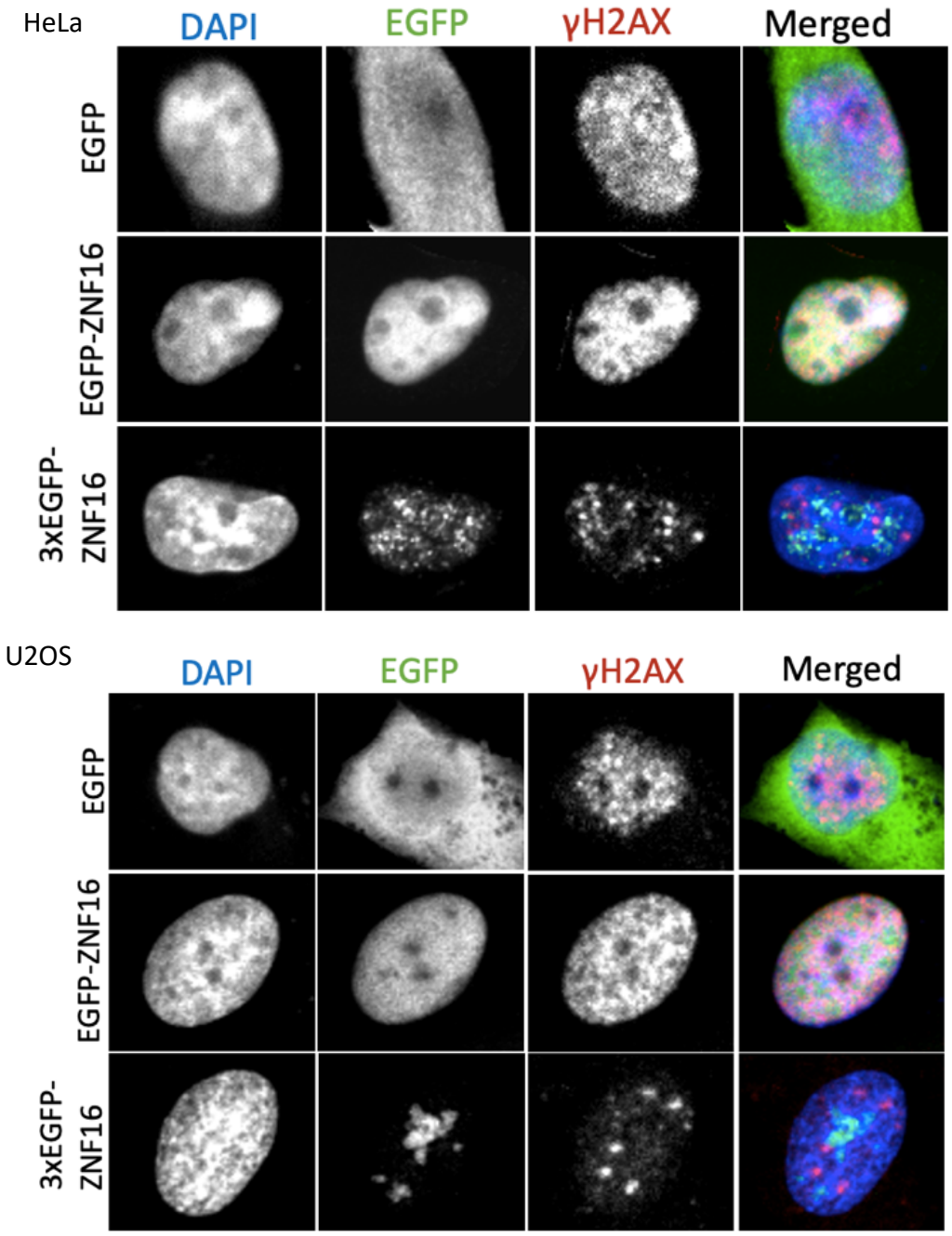


**Figure 12. Effect of ZNF16 overexpression on the DNA damage response of HeLa and U2OS cells treated with camptothecin.** HeLa TetON and U2OS cells were transiently transfected with the indicated plasmids. Before fixation, cells were treated with 10 μM camptothecin for four hours. The cells were fixed twenty-four hours after transfection and immunostained with antibodies against EGFP and the DNA damage marker γH2AX. Cells were then visualized by confocal microscopy.

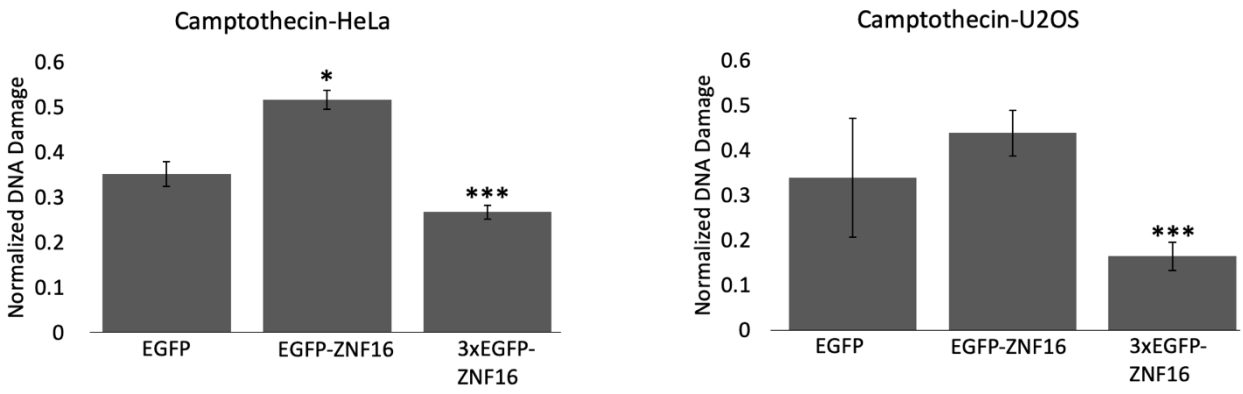


**Figure 13. Effect of ZNF16 overexpression on the DNA damage response of HeLa and U2OS cells treated with camptothecin.** Quantification of gH2AX intensity after transfection with exogenous ZNF16. gH2AX intensity was quantified in immunofluorescence images obtained as described in Figure X using ImageJ. Briefly, DAPI signal was used to delineate the nucleus of each cell and intensity of gH2AX was measured per nucleus and normalized to DAPI. (n=30, 10 cells from 3 trials) (*$p<0.5$, *** $p<0.001$)

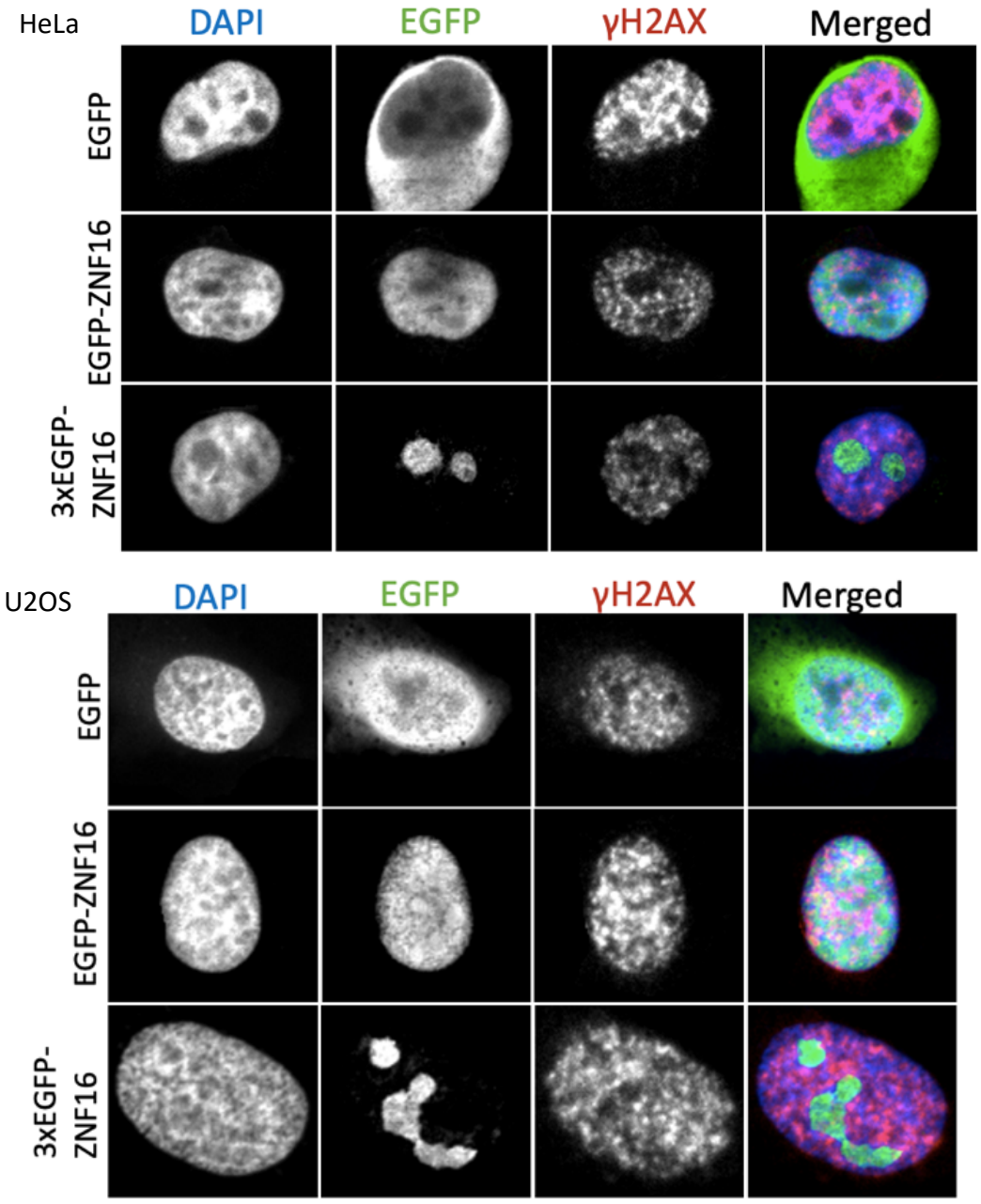


**Figure 14. Effect of ZNF16 overexpression on the DNA damage response of HeLa and U2OS cells treated with x-ray.** HeLa TetON and U2OS cells were transiently transfected with the indicated plasmids. Before fixation, cells were treated with 5Gy x-ray. The cells were fixed twenty-four hours after transfection and immunostained with antibodies against EGFP and the DNA damage marker γH2AX. Cells were then visualized by confocal microscopy.

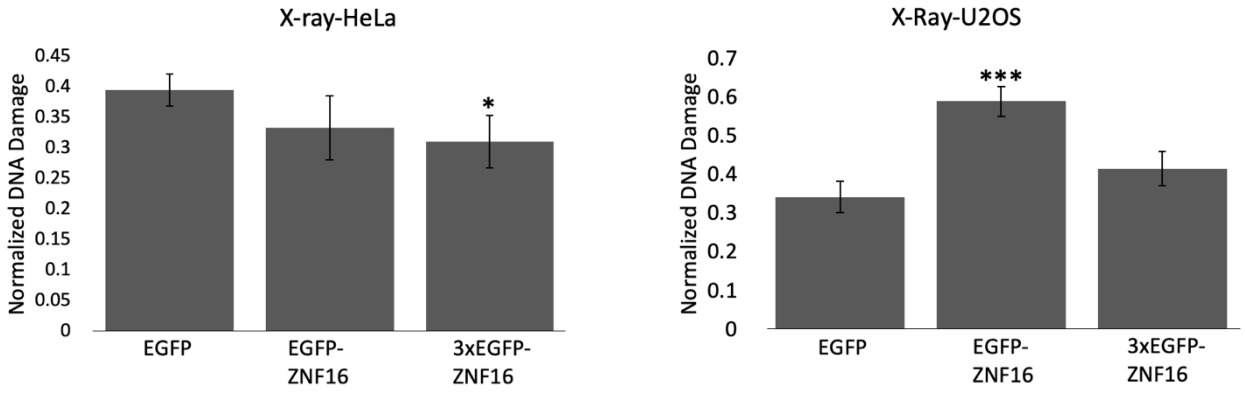


**Figure 15. Effect of ZNF16 overexpression on the DNA damage response of HeLa and U2OS cells treated with x-ray.** Quantification of gH2AX intensity after transfection with exogenous ZNF16. gH2AX intensity was quantified in immunofluorescence images obtained as described in Figure X using ImageJ. Briefly, DAPI signal was used to delineate the nucleus of each cell and intensity of gH2AX was measured per nucleus and normalized to DAPI. (n=30, 10 cells from 3 trials) (*p<0.5, *** p<0.001)

| | HeLa | | U2OS | |
|---|---|---|---|---|
| | EGFP-ZNF16 | 3xEGFP-ZNF16 | EGFP-ZNF16 | 3xEGFP-ZNF16 |
| DMSO | 1.009 | 1.370 * | 0.810 * | 0.677 *** |
| Cisplatin | 1.456 * | 1.753 ** | 0.918 | 0.430 *** |
| Camptothecin | 1.466 * | 0.759 *** | 1.294 | 0.486 *** |
| X-ray | 0.842 | 0.785 * | 1.722 *** | 1.213 |

Increased DNA Damage

Decreased DNA Damage

**Figure 16. Compiled DNA Damage.** Table indicates fold difference of DNA Damage compared to the EGFP control and significance. (*p<0.5, **p<0.01, *** p<0.001)

*Specific Aim 2: Examine if ZNF16 is involved in nucleolar structure or rRNA synthesis.*

Based on our results showing an enrichment for ZNF16 at the nucleolus (Figures 3 and 5-7), we decided to test whether ZNF16 has a role at the nucleolus. Other zinc finger proteins have been linked to nucleolar morphology (Israeli et al., 1997), pre-rRNA expression (Galcheva-Gargova et al., 1998), and processing (Miyazawa et al., 2014). In this aim I have designed experiments to test potential roles for ZNF16 in these functions.

*Nucleolar localization of ZNF16 is dependent on continuous rRNA transcription*

As previously mentioned, the nucleolus has several sub-sections, representing different areas of function and related proteins (Shaw and Jordan, 1995). When the nucleolus is exposed to stress by inhibiting rRNA transcription, proteins associated with rRNA transcription or processing delocalize to the nucleoplasm (Sirri et al., 2008), while the permanent protein residents remain in the nucleolus (Pederson, 2011). To inhibit rRNA transcription, cells were treated with 40 μM actinomycin D (AMD) and control cells were treated with vehicle (DMSO) for four hours before fixation. Actinomycin D is a known DNA intercalating agent (Mischo et al., 2005) which prevents the elongation of growing RNA strands by RNA polymerases. Ribosomal or nucleolar RNA synthesis is particularly sensitive to the presence of actinomycin D (Sobell, 1985). At the concentrations used in these experiments, actinomycin D inhibits ribosomal RNA synthesis by RNA polymerase I without affecting RNA synthesis by other RNA polymerases (Perry, 1963).

Nucleolar protein, Ki67 was used both as a marker of the nucleoli and as an marker for nucleolar stress, as it is shuttled from dense fibrillar centers in the nucleoli (MacCallum and Hall, 2000) to the nucleoplasm in response to actinomycin D induced nucleolar stress.

We began by examining the response of endogenous ZNF16 to nucleolar stress in both cell lines. After treatment with AMD, previously observed concentration of Ki67 in the nucleoli disappeared, as expected, as did the observed enrichment of ZNF16 in the nucleoli suggesting that it translocated to the nucleoplasm (Figure 17).

ZNF16 distribution was quantified in the micrographs to determine the level of delocalization. Because nucleolar structure breaks down in the presence of AMD, we cannot quantify the delocalization of ZNF16 using nucleolar boundaries like we did when we quantified the nucleolar enrichment of ZNF16. To quantify the delocalization of ZNF16 we first established a baseline for each cell by taking the average signal values of the lowest 50 data points from the plot profile derived from the line drawn through the nucleus to create a baseline. Then, we normalized all points to that baseline to account for cell-to-cell variability. We then found the percentage of data points that were 20% or higher above that baseline. This was done for a sample of cells to show there are more points 20% over the baseline in cells treated with DMSO indicating more points of enrichment compared to cells treated with AMD where the proteins have delocalized and therefor produce a more dispersed and even group of signal points.

We see this trend with Ki67, in Figure 18, which was expected based on the reports of Ki67 delocalizing from the nucleoli when rRNA transcription is halted, as well as with ZNF16 in both cell lines. This suggests that the enrichment of ZNF16 in the nucleoli we presented earlier is dependent on rRNA transcription, parallel to Ki67.

*Exogenous ZNF16 delocalizes from nucleoli when rRNA transcription is inhibited*

Next, we tested whether transiently expressed exogenous ZNF16, originally localized in the nucleoli, changes localization in response to nucleolar stress. HeLa and U2OS cells

overexpressing ZNF16 were treated with actinomycin D as described and processed for immunofluorescence microscopy (Figure 19 and 20). Interestingly, these results show that nucleolar ZNF16 delocalizes from the nucleoli to the nucleoplasm in a similar pattern as Ki67 in both cell lines. Here the phenomenon is even more pronounced, specifically in cells transfected with the 3XEGFP-ZNF16 plasmid, which displays a clear nucleolar localization, delocalized to the nucleoplasm after AMD treatment. These samples were quantified as previously mentioned with endogenous ZNF16 and the data for both cell lines indicates that exogenous ZNF16, previously localized in the nucleoli, delocalizes, like Ki67, to the nucleoplasm after the treatment of AMD (Figure 21).

The delocalization pattern of ZNF16 in response to the halting of rRNA transcription due to the presence of AMD was conserved when tested with both endogenous and exogenous ZNF16. These results indicate that ZNF16 is a temporary resident of the nucleoli whose localization is dependent on rRNA transcription, which suggests ZNF16 might be involved in rRNA transcription or processing.

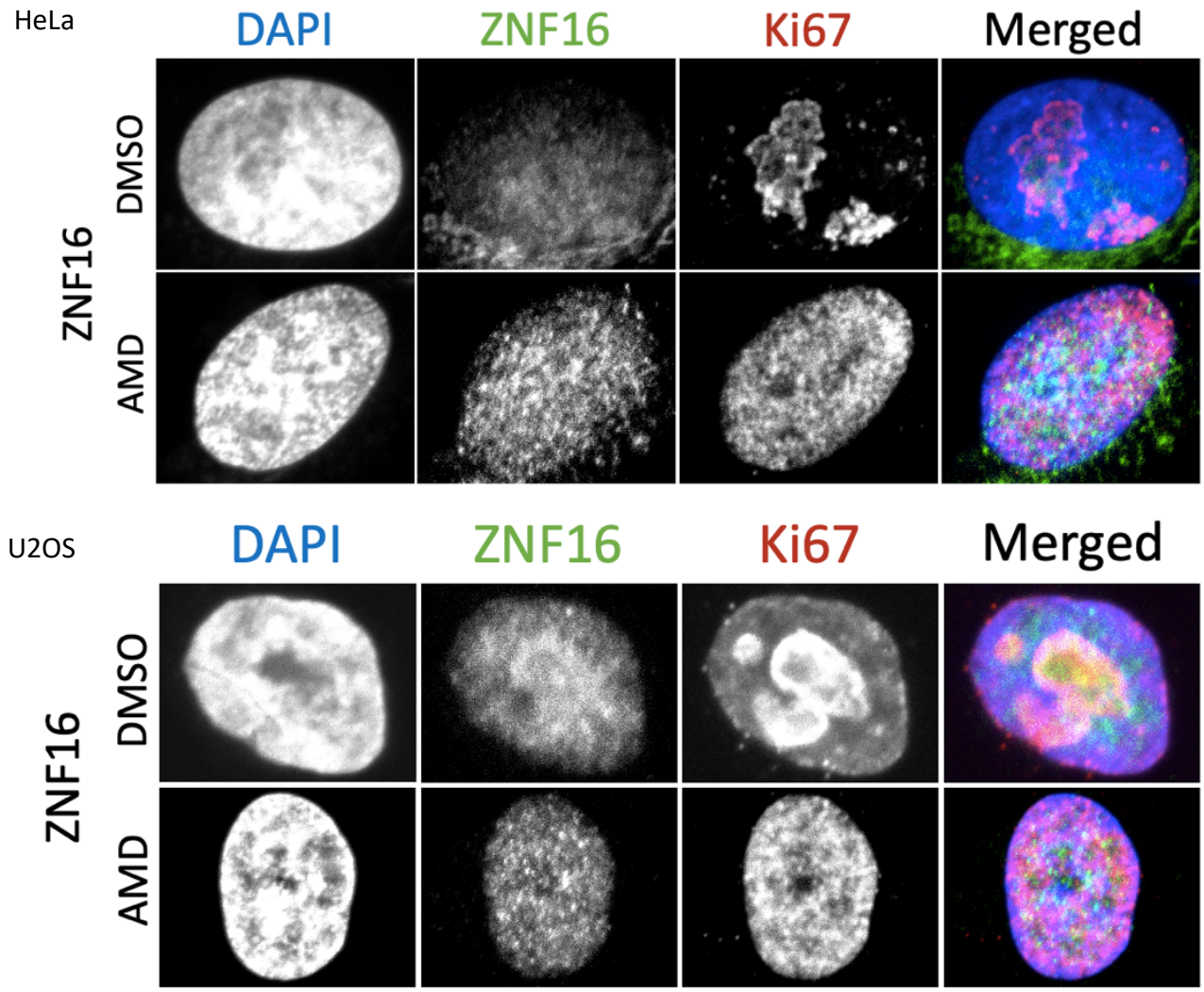


**Figure 17. Delocalization of endogenous ZNF16 from the nucleoli in response to actinomycin D induced nucleolar stress in HeLa and U2OS cells.** HeLa and U2OS cells were treated with 40 μM AMD, four hours before fixation. The cells were fixed and immunostained with antibodies against ZNF16 and the nucleolar marker Ki67 and visualized by confocal microscopy.

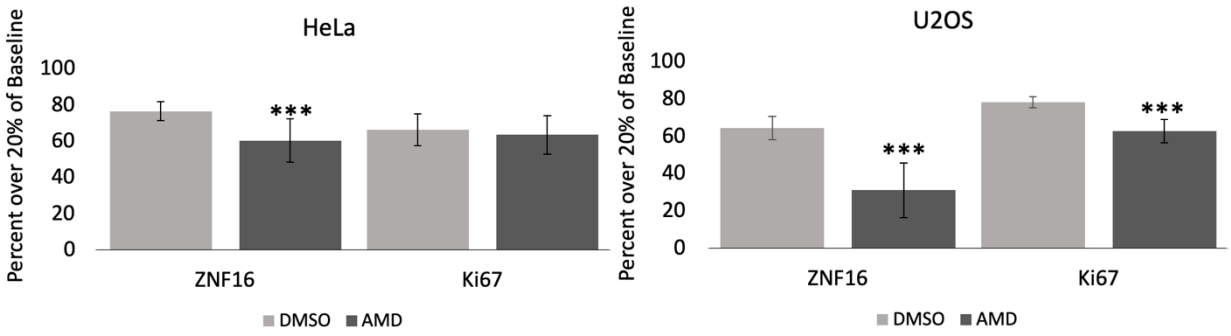


**Figure 18. Delocalization of endogenous ZNF16 from the nucleoli in response to actinomycin D induced nucleolar stress in HeLa and U2OS cells.** Hela and U2OS cells were fixed and immunostained with antibodies against ZNF16 and the nucleolar marker Ki67 and visualized by confocal microscopy. Image J was then used to draw a line through each cell resulting in signal points across the line. A baseline was created by taking the average signal values of the lowest 50 data points. The percentage of data points that were 20% or higher above that baseline was then calculated to show which samples have more points 20% over the baseline, indicating more points of enrichment compared to fewer points 20% over the baseline, indicating a more dispersed and even group of signal points. (*** $p<0.001$)

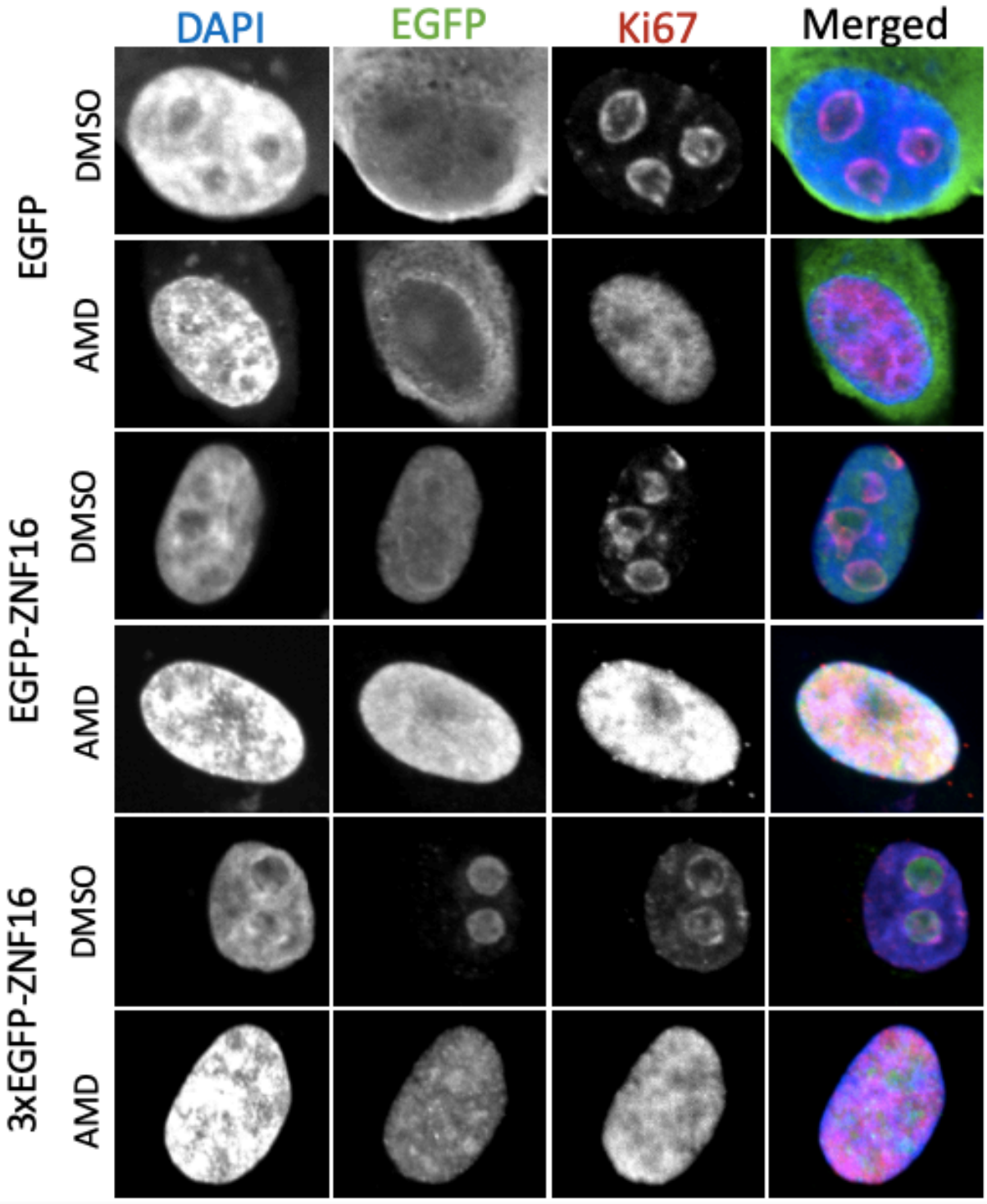


**Figure 19. Delocalization of transient exogenous ZNF16 from the nucleoli in response to actinomycin D (AMD) induced nucleolar stress.** HeLa TetON cells were transiently transfected with the indicated plasmids. Cells were treated with 40 μM AMD four hours before fixation. The cells were fixed twenty-four hours after transfection and immunostained with antibodies against EGFP and the nucleolar marker Ki67 and visualized by confocal microscopy.

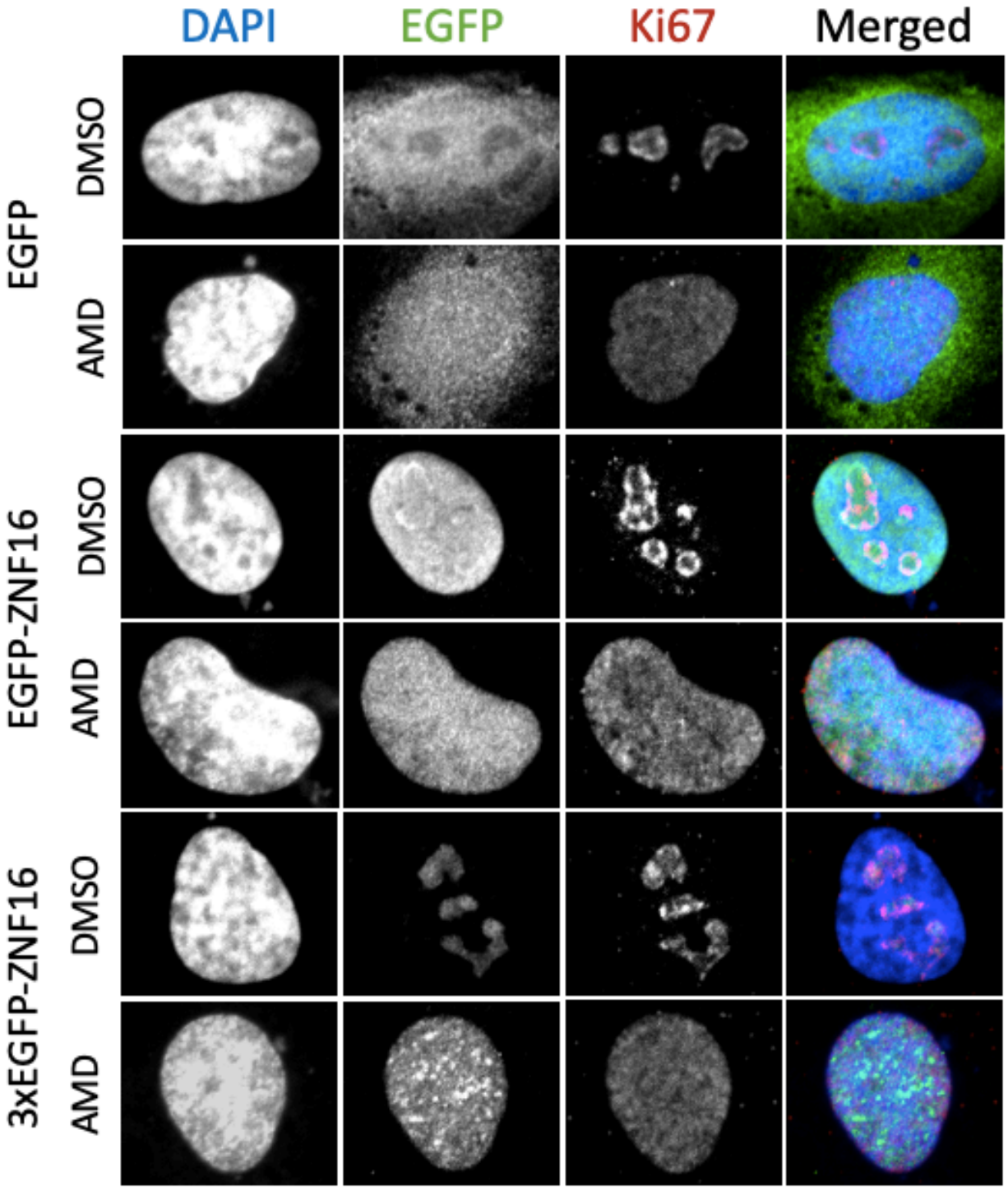


**Figure 20. Delocalization of transiently expressed exogenous ZNF16 from the nucleoli in response to actinomycin D (AMD) induced nucleolar stress.** U2OS cells were transiently transfected with the indicated plasmids. Cells were treated with 40 μM AMD four hours before fixation. The cells were fixed twenty-four hours after transfection and immunostained with antibodies against EGFP and the nucleolar marker Ki67 and visualized by confocal microscopy.

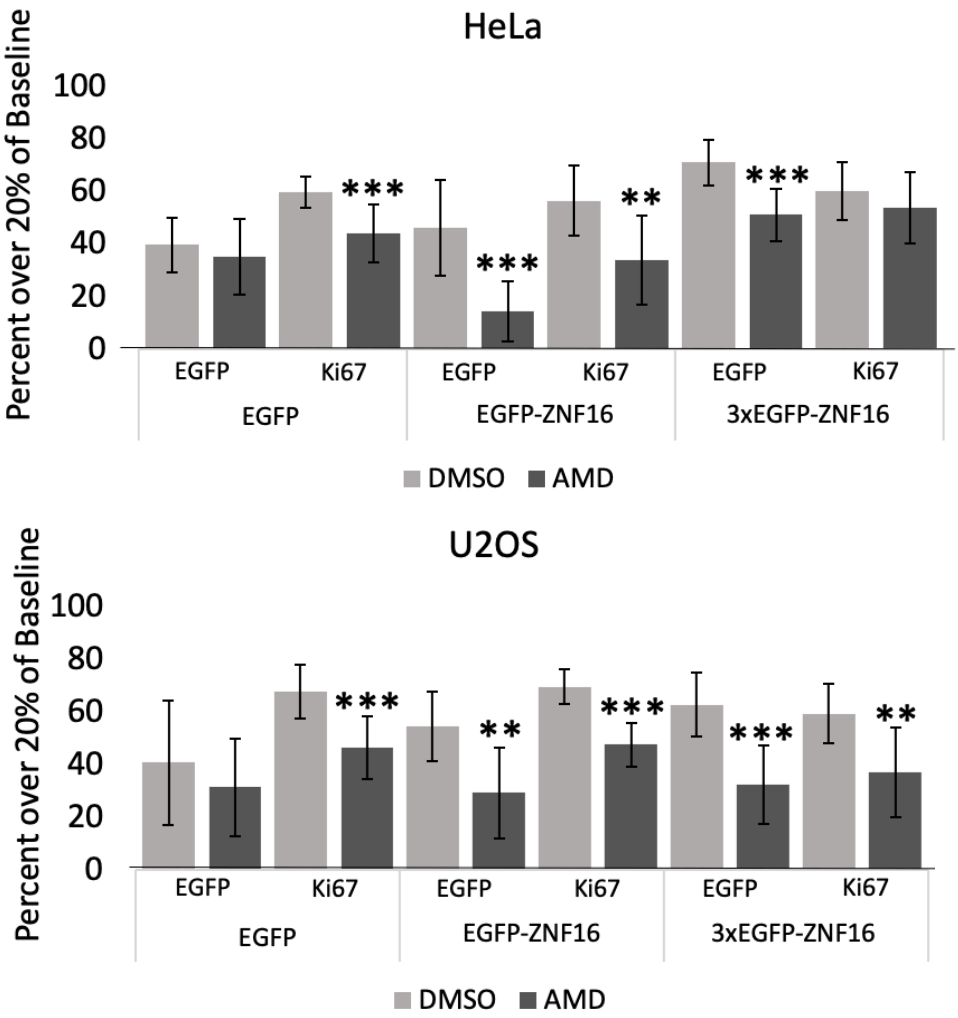


**Figure 21. Delocalization of transient exogenous ZNF16 from the nucleoli in response to actinomycin D (AMD) induced nucleolar stress.** HeLa and U2OS cells were cultured for 24 hours with the transfected plasmids and were then fixed and immunostained with antibodies against GFP and the nucleolar marker Ki67 and visualized by confocal microscopy. Image J was then used to draw a line through each cell resulting in signal points across the line. A baseline was created by taking the average signal values of the lowest 50 data points. The percentage of data points that were 20% or higher above that baseline was then calculated to show which samples have more points 20% over the baseline, indicating more points of enrichment compared to fewer points 20% over the baseline, indicating a more dispersed and even group of signal points. (*** $p<0.001$)

*Overexpression of ZNF16 in the nucleoli increases rRNA transcription*

In order to test a potential link between ZNF16 and rRNA synthesis, we implemented a luciferase assay using plasmid pHrD-IRES-Luc which contains an rDNA promoter followed by a luciferase reporter (Ghoshal et al., 2004). As a control we used plasmid pIRES-Luc, a luciferase reporter plasmid under the control of a minimal CMV promoter. Plasmids pHrD-IRES-Luc and pIRES-Luciferase were separately transfected in HeLa and U2OS cells with either EGFP, EGFP-ZNF16, or 3xEGFP-ZNF16 to test the effects of overexpressed exogenous ZNF16 on the transcription activity of the rRNA promoter.

Although both EGFP-ZNF16 and 3xEGFP-ZNF16 increase transcription in HeLa cells, it is interesting to note that 3xEGFP-ZNF16, which localizes in the nucleoli, increases transcription at dramatically higher levels (Figure 22A). In U2OS cells we see this same significant increase in transcription of the rDNA promoter when ZNF16 is overexpressed in the nucleoli (Figure 23A) Importantly, the transcriptional activation seems to be specific to the rDNA promoter, since ZNF16 overexpression does not increase transcription by the minimal CMV promoter (Figures 22B and 23B).

These results suggest that ZNF16 promotes rRNA transcription, specifically when overexpressed in the nucleolus. This potential function could be further studied through optimized knockdown assays to ascertain how the knockdown of ZNF16 may affect the transcription of rDNA via the rDNA promoters. Additionally, the role of ZNF16 in rRNA transcription can be explored by measuring the levels of pre-rRNA in the cell after overexpression and depletion of ZNF16 using qPCR assays.

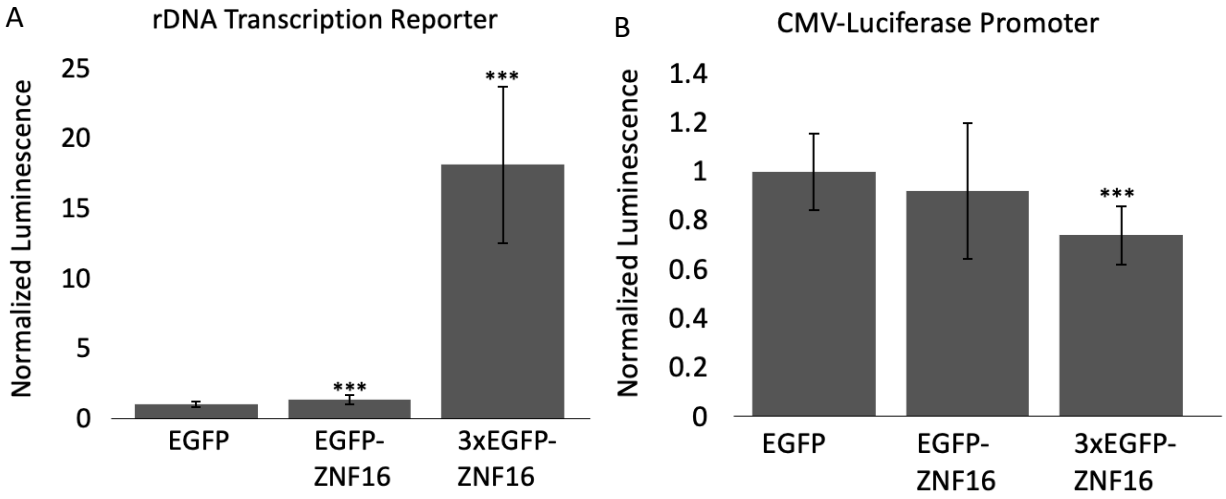


**Figure 22. Nucleolar exogenous ZNF16 increases rRNA transcriptional activity of an rDNA promoter observed by a luciferase reporter.** HeLa TetON cells were transiently transfected with the indicated plasmids and (A) pHrD-IRES-Luc or (B) pIRES-Luciferase. After forty-eight hours, luminescence was measured. The graphs represent the mean and standard deviation from five independent assays. (*** $p<0.001$)

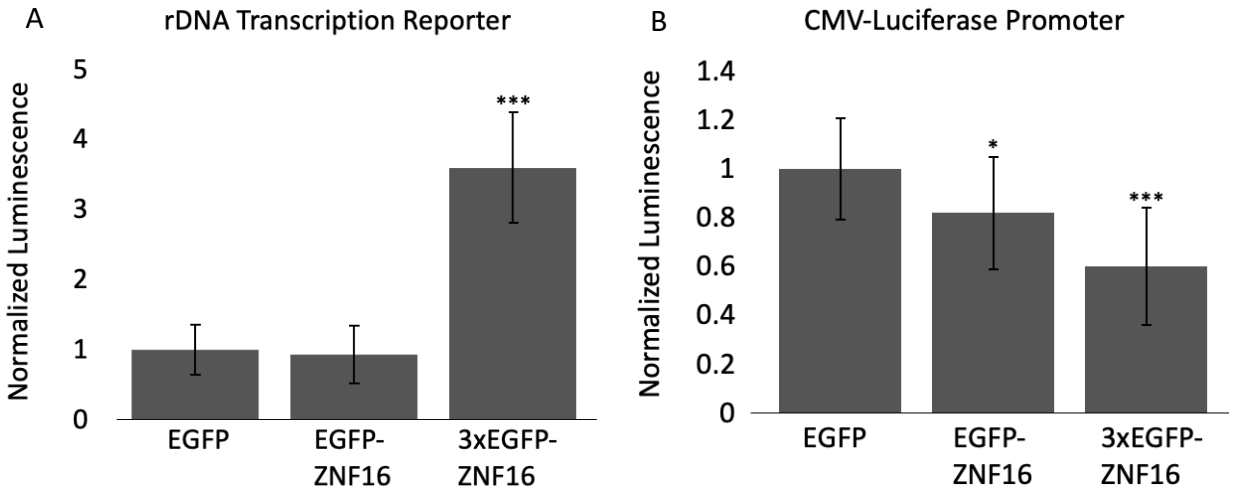


**Figure 23. Nucleolar exogenous ZNF16 increases rRNA transcriptional activity of an rDNA promoter observed by a luciferase reporter.** U2OS cells were transiently transfected with the indicated plasmids and (A) pHrD-IRES-Luc or (B) pIRES-Luciferase. After forty-eight hours, luminescence was measured. The graphs represent the mean and standard deviation from five independent assays. (*** $p<0.001$)

# CHAPTER 5: CONCLUSION AND FUTURE DIRECTIONS

ZNF16 is an understudied gene that has been linked to processes such as blood cell differentiation (Peng et al., 2006) and cell proliferation (Díaz-Martínez et al., 2014; Li et al., 2011). However, the details of ZNF16 function are limited and its ubiquitous expression in many cell lines hints at a more universal role. Based on the localization of ZNF16 in the nucleus or nucleolus (Deng et al., 2009; Thul et al., 2017), it is possible ZNF16 could have a role in nucleolar structure, ribosome synthesis and processing, or the DNA damage response. This research looked to identify a potential role of ZNF16 in these processes.

Assays completed in this study show exogenous and endogenous ZNF16 localizing to the nucleus and nucleoli (Figures 3-7). Interestingly, the localization of exogenous ZNF16 depends on the tag utilized, with EGFP-ZNF16 localizing in the nucleus and 3xEGFP-ZNF16 mainly localizing in the nucleolus. Using relatively larger tags, such as GFP, can sometimes alter the localization of proteins, however because the endogenous ZNF16 localizes to both the nucleus and nucleoli, we believe that both localizations are correct and that different tags favor or hinder specific localizations. It is interesting to note that 3xEGFP-ZNF16 localizes to other subnuclear structures in a fraction of the cells, in addition to the nucleoli. It will be interesting to test whether this change in localization is due to progression through the cell cycle, since the experiments were done in asynchronous cells.

A potential role for ZNF16 in DNA damage was also explored as seen in Figures 8-16, inspired by other zinc finger proteins playing roles in DNA damage or repair. As previously mentioned, the changes observed in the response to DNA damage varied by cell line and type of DNA damaging agent, indicating that ZNF16 is not likely to have a conserved role in this response. One notable exception is the significant decrease in camptothecin-induced DNA

damage in both HeLa and U2OS cells overexpressing ZNF16 in the nucleoli. Camptothecin is an inhibitor of Topoisomerase I, a protein enriched in the nucleolus, suggesting that nucleolar ZNF16 might be protective against damaged caused by inhibition of nucleolar proteins. These results indicate that while ZNF16 does not play a conserved or universal role in the DNA damage response, ZNF16 localized at the nucleolus might protect against DNA damage caused by inhibition of nucleolar proteins.

We next studied the role of ZNF16 at the nucleolus. Overexpression of ZNF16 does not seem to have a major effect on nucleolar structure (Figure 6), but ZNF16 delocalizes from the nucleoli to the nucleoplasm as a response to actinomycin D induced rRNA transcription inhibition (Figures 17-21). The delocalization of ZNF16 in response to this nucleolar stress suggests that ZNF16 is involved in the synthesis or processing of rRNA, as proteins involved with these processes often delocalize under nucleolar stress, such as the RNA polymerase I transcriptional inhibition caused by AMD (Boulon et al., 2010). Further testing of a potential role for ZNF16 in the nucleolus showed that overexpression of ZNF16, particularly nucleolar 3xEGFP-ZNF16, increased transcription by an rDNA promoter (Figures 22 and 23). These data could suggest that ZNF16 acts as a rDNA transcription factor when localized to the nucleoli.

Taken together, these results indicate a role for ZNF16 in the nucleolus, potentially as an rRNA transcription factor. Further study of this role will be performed by siRNA knockdown assays to further understand the mechanisms at play. Additionally, assays to measure the effects of ZNF16 expression on rDNA transcription, such as measuring pre-rRNA levels in cells with overexpression and knockdown of ZNF16 through qPCR methods will allow us to measure the effect of ZNF16 levels on endogenous rRNA expression. Further study of this novel role for ZNF16 in cancer and non-cancer cell lines may shed light on the nucleolar-cancer connection.

REFERENCES

**Basu, A. and Krishnamurthy, S.** (2010). Cellular responses to cisplatin-induced DNA damage. *J. Nucleic Acids* **2010**,.

**Boulon, S., Westman, B. J., Hutten, S., Boisvert, F. M. and Lamond, A. I.** (2010). The Nucleolus under Stress. *Mol. Cell* **40**, 216–227.

**Brayer, K. J. and Segal, D. J.** (2008). Keep your fingers off my DNA: Protein-protein interactions mediated by C2H2 zinc finger domains. *Cell Biochem. Biophys.* **50**, 111–131.

**Brown, R. S.** (2005). Zinc finger proteins: Getting a grip on RNA. *Curr. Opin. Struct. Biol.* **15**, 94–98.

**Cassandri, M., Smirnov, A., Novelli, F., Pitolli, C., Agostini, M., Malewicz, M., Melino, G. and Raschellà, G.** (2017). Zinc-finger proteins in health and disease. *Cell Death Discov.* **3**, 17071.

**Chen, J., Li, X.-B., Su, R., Song, L., Wang, F. and Zhang, J.-W.** (2014). ZNF16 (HZF1) promotes erythropoiesis and megakaryocytopoiesis via regulation of the c- KIT gene. *Biochem. J.* **458**, 171–183.

**Cheng, Y., Liang, P., Geng, H., Wang, Z., Li, L., Cheng, S. H., Ying, J., Su, X., Ng, K. M., Ng, M. H. L., et al.** (2012). A novel 19q13 nucleolar zinc finger protein suppresses tumor cell growth through inhibiting ribosome biogenesis and inducing apoptosis but is frequently silenced in multiple carcinomas. *Mol. Cancer Res.* **10**, 925–936.

**Collins, T., Stone, J. R. and Williams, A. M. Y. J.** (2001). All in the Family : the BTB / POZ , KRAB , and SCAN Domains. *Mol. Cell. Biol.* **21**, 3609–3615.

**De Bont, R. and van Larebeke, N.** (2004). Endogenous DNA damage in humans: A review of quantitative data. *Mutagenesis* **19**, 169–185.

**Deng, M. J., Li, X. B., Peng, H. and Zhang, J. W.** (2009). Identification of the trans-activation domain and the nuclear location signals of human zinc finger protein HZF1 (ZNF16). *Mol. Biotechnol.* **44**, 83–89.

**Díaz-Martínez, L. A., Karamysheva, Z. N., Warrington, R., Li, B., Wei, S., Xie, X., Roth, M. G. and Yu, H.** (2014). Genome-wide siRNA screen reveals coupling between mitotic apoptosis and adaptation. *EMBO J.* **33**, 1960–1976.

**Dousset, T., Wang, C., Verheggen, C., Chen, D., Hernandez-Verdun, D. and Huang, S.** (2000). Initiation of nucleolar assembly is independent of RNA polymerase I transcription. *Mol. Biol. Cell* **11**, 2705–2717.

**Farley-Barnes, K. I., McCann, K. L., Baserga, S. J., Ogawa, L. M., Merkel, J. and Surovtseva, Y. V.** (2018). Diverse Regulators of Human Ribosome Biogenesis Discovered by Changes in Nucleolar Number. *Cell Rep.* **22**, 1923–1934.

**Friedberg, E. C.** (2003). DNA damage and repair. *Nature* **421**, 436–440.

**Galcheva-Gargova, Z., Gangwani, L., Konstantinov, K. N., Mikrut, M., Theroux, S. J., Enoch, T. and Davis, R. J.** (1998). The Cytoplasmic Zinc Finger Protein ZPR1 Accumulates in the Nucleolus of Proliferating Cells. *Mol. Biol. Cell* **9**, 2963–2971.

**Ghoshal, K., Majumder, S., Datta, J. and Motiwala, T.** (2004). Role of Human Ribosomal RNA (rRNA) Promoter Methylation and of Methyl-CpG-binding Protein MBD2 in the Suppression of rRNA Gene Expression. *J Cell Biochem* **99**, 671–678.

**Graveline, R., Marcinkiewicz, K., Choi, S., Paquet, M., Wurst, W., Floss, T. and David, G.** (2017). The Chromatin-Associated Phf12 Protein Maintains Nucleolar Integrity and Prevents Premature Cellular Senescence. *Mol. Cell. Biol.* **37**, 1–14.

**Grummt, I.** (2003). Life on a planet of its own: Regulation of RNA polymerase I transcription in the nucleolus. *Genes Dev.* **17**, 1691–1702.

**Hein, N., Hannan, K. M., George, A. J., Sanij, E. and Hannan, R. D.** (2013). The nucleolus: An emerging target for cancer therapy. *Trends Mol. Med.* **19**, 643–654.

**Hernandez-Verdun, D., Roussel, P., Thiry, M., Sirri, V. and Lafontaine, D. L. J.** (2010). The nucleolus: Structure/function relationship in RNA metabolism. *Wiley Interdiscip. Rev. RNA* **1**, 415–431.

**Hruban, R. H., Yardley, J. H., Donehower, R. C. and Boitnott, J. K.** (1989). Taxol toxicity. Epithelial necrosis in the gastrointestinal tract associated with polymerized microtubule accumulation and mitotic arrest. *Cancer* **63**, 1944–1950.

**Huang, X. D., Wang, J. Y. J. and Lu, X.** (2008). Systems analysis of quantitative shRNA-library screens identifies regulators of cell adhesion. *BMC Syst. Biol.* **2**, 1–11.

**Israeli, D., Tessler, E., Haupt, Y., Elkeles, A., Wilder, S., Amson, R., Telerman, A. and Oren, M.** (1997). A novel p53-inducible gene, PAG608, encodes a nuclear zinc finger protein whose overexpression promotes apoptosis. *EMBO J.* **16**, 4384–4392.

**Iuchi, S.** (2001a). Three classes of C2H2 zinc finger proteins. *Cell. Mol. Life Sci.* **58**, 625–635.

**Iuchi, S.** (2001b). Cellular and Molecular Life Sciences Three classes of C 2 H 2 zinc finger proteins. *Cell. Mol. life Sci.* **58**, 625–635.

**Jackson, S. P. and Bartek, J.** (2009). The DNA-damage response in human biology and disease. *Nature* **461**, 1071–1078.

**Jarboui, M. A., Wynne, K., Elia, G., Hall, W. W. and Gautier, V. W.** (2011). Proteomic profiling of the human T-cell nucleolus. *Mol. Immunol.* **49**, 441–452.

**Klein, J. and Grummt, I.** (1999). Cell cycle-dependent regulation of RNA polymerase I transcription: The nucleolar transcription factor UBF is inactive in mitosis and early G1. *Proc. Natl. Acad. Sci. U. S. A.* **96**, 6096–6101.

**Lamond, A. I. and Earnshaw, W. C.** (1998). Structure and function in the Nucleus. *Science (80-. ).* **280**, 3–38.

**Li, X. B., Chen, J., Deng, M. J., Wang, F., Du, Z. W. and Zhang, J. W.** (2011). Zinc finger protein HZF1 promotes K562 cell proliferation by interacting with and inhibiting INCA1. *Mol. Med. Rep.* **4**, 1131–1137.

**Liu, X., Jin, E. Z., Zhi, J. X. and Li, X. Q.** (2011). Identification of HZF1 as a novel target gene of the MEF2 transcription factor. *Mol. Med. Rep.* **4**, 465–469.

**Lorenz, P., Dietmann, S., Wilhelm, T., Koczan, D., Autran, S., Gad, S., Wen, G., Ding, G., Li, Y., Rousseau-Merck, M. F., et al.** (2010). The ancient mammalian KRAB zinc finger gene cluster on human chromosome 8q24.3 illustrates principles of C2H2 zinc finger evolution associated with unique expression profiles in human tissues. *BMC Genomics* **11**,.

**MacCallum, D. E. and Hall, P. A.** (2000). The location of pKi67 in the outer dense fibrillary compartment of the nucleolus points to a role in ribosome biogenesis during the cell division cycle. *J. Pathol.* **190**, 537–544.

**Mayer, C. and Grummt, I.** (2005). Cellular stress and nucleolar function. *Cell Cycle* **4**, 1036–1038.

**Milas, L., Hunter, N. R., Kurdoglu, B., Mason, K. A., Meyn, R. E., Stephens, L. C. and Peters, L. J.** (1995). Kinetics of mitotic arrest and apoptosis in murine mammary and ovarian tumors treated with taxol. *Cancer Chemother. Pharmacol.* **35**, 297–303.

**Mischo, H. E., Hemmerich, P., Grosse, F. and Zhang, S.** (2005). Actinomycin D induces histone γ-H2AX foci and complex formation of γ-H2AX with Ku70 and nuclear DNA

helicase II. *J. Biol. Chem.* **280**, 9586–9594.
**Misteli, T.** (2001). Nuclear structure - Protein dynamics: Implications for nuclear architecture and gene expression. *Science (80-. ).* **291**, 843–847.
**Miyazawa, N., Yoshikawa, H., Magae, S., Ishikawa, H., Izumikawa, K., Terukina, G., Suzuki, A., Nakamura-Fujiyama, S., Miura, Y., Hayano, T., et al.** (2014). Human cell growth regulator Ly-1 antibody reactive homologue accelerates processing of preribosomal RNA. *Genes to Cells* **19**, 273–286.
**Mo, Y. Y., Yu, Y., Shen, Z. and Beck, W. T.** (2002). Nucleolar delocalization of human topoisomerase I in response to topotecan correlates with sumoylation of the protein. *J. Biol. Chem.* **277**, 2958–2964.
**Montanaro, L., Treré, D. and Derenzini, M.** (2008). Nucleolus, ribosomes, and cancer. *Am. J. Pathol.* **173**, 301–310.
**Najafabadi, H. S., Mnaimneh, S., Schmitges, F. W., Garton, M., Lam, K. N., Yang, A., Albu, M., Weirauch, M. T., Radovani, E., Kim, P. M., et al.** (2015). C2H2 zinc finger proteins greatly expand the human regulatory lexicon. *Nat. Biotechnol.* **33**, 555–562.
**Németh, A. and Grummt, I.** (2018). Dynamic regulation of nucleolar architecture. *Curr. Opin. Cell Biol.* **52**, 105–111.
**Nicolas, E., Parisot, P., Pinto-Monteiro, C., De Walque, R., De Vleeschouwer, C. and Lafontaine, D. L. J.** (2016). Involvement of human ribosomal proteins in nucleolar structure and p53-dependent nucleolar stress. *Nat. Commun.* **7**, 1–12.
**Olson, M. O. J.** (2004). Sensing cellular stress: another new function for the nucleolus? *Sci. STKE* **2004**, 1–4.
**Pederson, T.** (2011). The Nucleolus. *Cold Spring Harb. Perspect. Biol.* **3**, 185–212.
**Peltonen, K., Colis, L., Liu, H., Trivedi, R., Moubarek, M. S., Moore, H. M., Bai, B., Rudek, M. A., Bieberich, C. J. and Laiho, M.** (2014). A targeting modality for destruction of RNA polymerase I that possesses anticancer activity. *Cancer Cell* **25**, 77–90.
**Peng, H., Du, Z. W. and Zhang, J. W.** (2006). Identification and characterization of a novel zinc finger protein (HZF1) gene and its function in erythroid and megakaryocytic differentiation of K562 cells. *Leukemia* **20**, 1109–1116.
**Perry, R. P.** (1963). SELECTIVE EFFECTS OF ACTINOMYCIN D ON THE INTRACELLULAR DISTRIBUTION OF RNA SYNTHESIS IN TISSUE CULTURE CELLS. *Exp. Cell Res.* **406**, 400–406.
**Quin, J. E., Devlin, J. R., Cameron, D., Hannan, K. M., Pearson, R. B. and Hannan, R. D.** (2014). Targeting the nucleolus for cancer intervention. *Biochim. Biophys. Acta - Mol. Basis Dis.* **1842**, 802–816.
**Rancourt, A. and Satoh, M. S.** (2009). Delocalization of nucleolar poly(ADP-ribose) polymerase-1 to the nucleoplasm and its novel link to cellular sensitivity to DNA damage. *DNA Repair (Amst).* **8**, 286–297.
**Reimer, G., Raška, I., Tan, E. M. and Scheer, U.** (1987). Human autoantibodies: probes for nucleolus structure and function. *Virchows Arch. B Cell Pathol. Incl. Mol. Pathol.* **54**, 131–143.
**Rivera-León, R. and Gerbi, S. A.** (1997). Delocalization of some small nucleolar RNPs after actinomycin D treatment to deplete early pre-rRNAs. *Chromosoma* **105**, 506–514.
**Roos, W. P. and Kaina, B.** (2006). DNA damage-induced cell death by apoptosis. *Trends Mol. Med.* **12**, 440–450.
**Sancar, A., Lindsey-Boltz, L. A., Unsal-Kaçmaz, K. and Linn, S.** (2004). Molecular

mechanisms of mammalian DNA repair and the DNA damage checkpoints. *Annu. Rev. Biochem.* **73**, 39–85.

**Scheer, U. and Hock, R.** (1999). Structure and function of the nucleolus. *Curr. Opin. Cell Biol.* **11**, 385–390.

**Schiff, P. B., Fant, J. and Horwitz, S. B.** (1979). Promotion of microtubule assembly in vitro by taxol. *Nature* **277**, 665–7.

**Shaw, P. J. and Jordan, E. G.** (1995). The Nucleolus. *J. Cell Sci.* **2005**, 1335–1337.

**Sidik, H. and Talbot, W. S.** (2015). A zinc finger protein that regulates oligodendrocyte specification, migration and myelination in zebrafish. *Development* **142**, 4119–4128.

**Sirri, V., Urcuqui-Inchima, S., Roussel, P. and Hernandez-Verdun, D.** (2008). Nucleolus: The fascinating nuclear body. *Histochem. Cell Biol.* **129**, 13–31.

**Snyder, R. D. and Lachmann, P. J.** (1989). Differential effects of 5-azacytidine and 5-azadeoxycytidine on cytotoxicity, DNA-strand breaking and repair of X-ray-induced DNA damage in HeLa cells. *Mutat. Res. Lett.* **226**, 185–190.

**Sobell, H. M.** (1985). Actinomycin and DNA transcription. **82**, 5328–5331.

**Spector, D. L.** (2001). Nuclear domains. *J. Cell Sci.* **24**, 51–59.

**Su, L., Hershberger, R. J. and Weissman, I. L.** (1993). LYAR, a novel nucleolar protein with zinc finger DNA-binding motifs, is involved in cell growth regulation. *Genes Dev.* **7**, 735–748.

**Sun, Y., Atmadibrata, B., Yu, D., Wong, M., Liu, B., Ho, N., Ling, D., Tee, A. E., Wang, J., Mungrue, I. N., et al.** (2017). Upregulation of LYAR induces neuroblastoma cell proliferation and survival. *Cell Death Differ.* **24**, 1645–1654.

**Tafforeau, L., Zorbas, C., Langhendries, J.-L., Lafontaine, D. L. J., Mullier, R., Stamatopoulou, V., Mullineux, S.-T. and Wacheul, L.** (2013). The Complexity of Human Ribosome Biogenesis Revealed by Systematic Nucleolar Screening of Pre-rRNA Processing Factors. *Mol. Cell* **51**, 539–551.

**Thul, P. J., Akesson, L., Wiking, M., Mahdessian, D., Geladaki, A., Ait Blal, H., Alm, T., Asplund, A., Björk, L., Breckels, L. M., et al.** (2017). A subcellular map of the human proteome. *Science (80-. ).* **356**,.

**Trinkle-Mulcahy, L.** (2018). *Nucleolus: The Consummate Nuclear Body*. Elsevier Inc.

**Uhlén, M., Fagerberg, L., Hallström, B. M., Lindskog, C., Oksvold, P., Mardinoglu, A., Sivertsson, Å., Kampf, C., Sjöstedt, E., Asplund, A., et al.** (2015). Tissue-based map of the human proteome. *Science (80-. ).* **347**,.

**Urrutia, R.** (2003). KRAB-containing zinc-finger repressor proteins. *Genome Biol.* **4**,.

**Verheijen, R., Kuijpers, H. J. H., Schlingemann, R. O., Boehmer, A. L. M., Van Driel, R., Brakenhoff, G. J. and Ramaekers, F. C. S.** (1989). Ki-67 detects a nuclear matrix-associated proliferation-related antigen I. Intracellular localization during interphase. *J. Cell Sci.* **92**, 123–130.

**Wang, S., Cheng, Y., Du, W., Lu, L., Zhou, L., Wang, H., Kang, W., Li, X., Tao, Q., Sung, J. J. Y., et al.** (2013). Zinc-finger protein 545 is a novel tumour suppressor that acts by inhibiting ribosomal RNA transcription in gastric cancer. *Gut* **62**, 833–841.

**Warde-Farley, D., Donaldson, S. L., Comes, O., Zuberi, K., Badrawi, R., Chao, P., Franz, M., Grouios, C., Kazi, F., Lopes, C. T., et al.** (2010). The GeneMANIA prediction server: Biological network integration for gene prioritization and predicting gene function. *Nucleic Acids Res.* **38**, 214–220.

**Weaver, B. A.** (2014). How Taxol/paclitaxel kills cancer cells. *Mol. Biol. Cell* **25**, 2677–2681.

**Yano, K., Ueki, N., Oda, T., Seki, N., Masuho, Y. and Muramatsu, M. A.** (2000). Identification and characterization of human ZNF274 cDNA, which encodes a novel Kruppel-type zinc-finger protein having nucleolar targeting ability. *Genomics* **65**, 75–80.

**Zhang, P., Branson, O. E., Freitas, M. A. and Parthun, M. R.** (2016). Identification of replication-dependent and replication-independent linker histone complexes: Tpr specifically promotes replication-dependent linker histone stability. *BMC Biochem.* **17**, 1–16.

**Zhou, B. S. and Elledge, S. J.** (2000). The DNA damage response: putting checkpoints in perspective. *Nature* **408**, 433–439.

# VITA

Before completing her Master of Science in Biology at The University of Texas at El Paso, Chelsea George earned a Bachelor of Science in Biology with Minors in Chemistry and Spanish and a Comprehensive Sciences High School Teaching Licensure from The University of North Carolina at Greensboro. She has enjoyed science education for many years with experience as an intern & intern coordinator at the Hatteras Island Ocean Center, tutor and large group tutor for Math, Spanish, and a variety of Sciences at The University of North Carolina at Greensboro, student intern in several North Carolina high school science classes, student teacher teaching high school honors Chemistry, and as a TA for an introductory biology lab at The University of Texas at El Paso. She can be reached at chelsealgeorge@gmail.com.